



**UNIVERSIDAD DE INVESTIGACIÓN DE
TECNOLOGÍA EXPERIMENTAL YACHAY**

Escuela de Ciencias Físicas y Nanotecnología

**TÍTULO: Spatio-temporal chaos in continuous-time dynamical
networks**

Trabajo de integración curricular presentado como requisito para la
obtención del título de Físico

Autor:

David Nicolás Eraso Ortiz

Tutor:

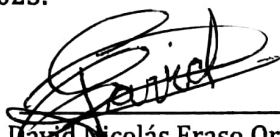
PhD. Cosenza Miceli Mario Giuseppe

Urququí, Diciembre 2023

AUTORÍA

Yo, **DAVID NICOLÁS ERASO ORTIZ**, con cédula de identidad 1716581721 declaro que las ideas, juicios, valoraciones, interpretaciones, consultas bibliográficas, definiciones y conceptualizaciones expuestas en el presente trabajo; así cómo, los procedimientos y herramientas utilizadas en la investigación, son de absoluta responsabilidad de el/la autora (a) del trabajo de integración curricular. Así mismo, me acojo a los reglamentos internos de la Universidad de Investigación de Tecnología Experimental Yachay.

Urcuquí, Diciembre 2023.



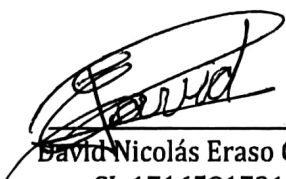
David Nicolás Eraso Ortiz
CI: 1716581721

AUTORIZACIÓN DE PUBLICACIÓN

Yo, **DAVID NICOLÁS ERASO ORTIZ**, con cédula de identidad 1716581721 cedo a la Universidad de Investigación de Tecnología Experimental Yachay, los derechos de publicación de la presente obra, sin que deba haber un reconocimiento económico por este concepto. Declaro además que el texto del presente trabajo de titulación no podrá ser cedido a ninguna empresa editorial para su publicación u otros fines, sin contar previamente con la autorización escrita de la Universidad.

Asimismo, autorizo a la Universidad que realice la digitalización y publicación de este trabajo de integración curricular en el repositorio virtual, de conformidad a lo dispuesto en el Art. 144 de la Ley Orgánica de Educación Superior

Urcuquí, Diciembre 2023.



David Nicolás Eraso Ortiz
Ci: 1716581721

Dedication

I dedicate all this work and that carried out throughout my career, first, to my parents, Guido Eraso and Monika Ortiz, who taught me the true meaning of perseverance and love, who instilled in me that no matter how far arrives never ceases to be simple and authentic. To my grandmother, Mariela Murcia, for her immeasurable love that gives her grace in my life. And to Jannys Valles, my anchor and guiding light on this journey: her unwavering love and her trust in me have made all the difference.

Acknowledgements

First and foremost, I wish to express my deepest gratitude to my thesis advisor, Dr. Mario Cosenza, for his invaluable guidance, expertise, and patience throughout this journey. His wisdom and knowledge were fundamental to the completion of this work. In addition to being a person whom I deeply admire for his values and contributions to human knowledge.

To my siblings, Laura and Jorge, for their unwavering support, encouragement, and the occasional distractions that kept me grounded.

A special acknowledgment to my closest friends, Francisco E and Jose M, who stood by me during the highs and lows, always offering a listening ear and comforting words.

To my university mates, Juan Diego and Alejandro, whose camaraderie made the academic challenges more bearable and the successes even more memorable.

Lastly, to all the passionate educators who have imparted the wonders of physics upon me: Helga D, Vladimir, and Henry. Your dedication and enthusiasm have ignited a lifelong passion in me, and I am eternally grateful.

Resumen

El caos colectivo es un comportamiento colectivo no trivial que consiste en la persistencia del comportamiento caótico a nivel macroscópico en sistemas de elementos dinámicos en interacción que poseen un comportamiento periódico individual. Este fenómeno se manifiesta por la existencia de supertransitorios caóticos en el tiempo antes de que el sistema sincronice en su atractor periódico. Investigamos el papel del rango de interacciones en la emergencia del caos colectivo en redes dinámicas espacio-temporales considerando una red en anillo de elementos acoplados con un rango variable de interacciones. Encontramos un rango crítico de alrededor del 20% del tamaño del sistema, por encima del cual no se observa caos colectivo y la red inevitablemente sincroniza en la órbita periódica de los elementos constitutivos. Descubrimos que el caos colectivo no ocurre en redes globalmente acopladas de sistemas de tiempo continuo cuando la intensidad del parámetro de acoplamiento está por debajo de cierto valor crítico. Caracterizamos el estado sincronizado de un sistema a través de una medida de la desviación estándar de los estados de los elementos. Nuestros resultados indican que la topología de conectividad de la red, así como la fuerza del acoplamiento entre los elementos, son factores cruciales para la emergencia del caos colectivo en sistemas dinámicos espacio-temporales.

Palabras Clave: Sistemas complejos; redes globalmente acopladas; caos transitorio; caos colectivo; sincronización; redes dinámicas.

Abstract

Collective chaos is a nontrivial collective behavior consisting of the persistence of chaotic behavior at the macroscopic level in systems of interacting dynamical elements possessing individual periodic behavior. This phenomenon is manifested by the existence of chaotic supertransients in time before the system synchronizes into its period attractor. We investigate the role of the range of interactions on the emergence of collective chaos in spatiotemporal dynamical networks by considering ring network of coupled elements with a varying range of interactions. We encounter a critical range of about 20% of the system size above which no collective chaos is observed and the network invariably synchronizes in the periodic orbit of the constitutive elements. We find that collective chaos does not occur in globally coupled networks of continuous time systems when the intensity of the coupling parameter is below some critical value. We characterize the synchronized state of a system through a measure of the standard deviation of the states of the elements. Our results indicate that the topology of connectivity of the network, as well as the strength of coupling between the elements, are crucial factors for the emergence of collective chaos in spatiotemporal dynamical systems.

Keywords: Complex systems; globally coupled networks; transient chaos; collective chaos; synchronization; dynamical networks.

Contents

1	Introduction	13
1.1	Research problem	14
1.2	Objectives	14
1.2.1	General objective	14
1.2.2	Specific objectives	14
2	Theoretical framework	15
2.1	Supertransient chaos	15
2.2	Collective stable chaos	17
2.3	Globally Coupled Systems	18
2.4	Elementary chaotic flow	19
3	Spatiotemporal chaos in continuous-time dynamical networks	21
3.1	Numerical solution of Linz-Sprott's Equations	21
3.2	Globally coupled network	22
3.2.1	Collective synchronization of periodic orbits	23
3.2.2	Characterizing synchronization.	25
3.3	Networks with varying range of interactions	27
3.3.1	Synchronization and range of interaction	30
4	Conclusions	33
	Bibliography	35
	Appendices	38
A	Python code for globally coupled network of Linz-Sprott equations	41

List of Figures

2.1	States $x_n(i)$ of $N = 50$ maps as functions of discrete time n for the system Eqs. (2.1) with parameter values $a = 1.752$ and $\epsilon = 1.05 \times 10^{-3}$, plotted every 90 time steps. Color code is as follows: if $ x_n(i+1) - x_n(i) < 0.3$ the i th site is white, otherwise it is black. Taken from Ref. ¹	16
2.2	Semi-log plots of the average transient times T versus the logarithm of the system size N of the system Eqs. (2.1), for different values of the coupling strength ϵ . Fixed parameter $a = 1.752$. The symbols indicate different values, ranging from $\epsilon = 0.0011$ (open circles) to $\epsilon = 0.005$ (full black circles). Taken from Ref. ¹	16
2.3	Left: Local map Eq. 2.2 with $a = 0.1$, $b = 2.5$ and $c = 0$. Right: Bifurcation diagram of map Eq. 2.2 as a function of b for fixed parameter values $a = 0.1$ and $c = 0$. The values of the period-3 superstable orbit are indicated by black dots.	17
2.4	Bifurcation diagram of the mean field H_t and the average dispersion $\langle \sigma \rangle$ as functions of ϵ for the system Eqs. (2.1) with size $N = 10^3$. For each value of ϵ 10^3 values of H_t are plotted, after discarding 10^4 transients. The quantity $\langle \sigma \rangle$ is calculated as the average of 10^3 values of σ_t , after discarding 10^4 transients. Taken from Ref. ²	18
2.5	View of the chaotic attractor of the system Eqs. (2.6) for the parameter value $a = 0.6$. Initial conditions are $\ddot{x} = \dot{x} = x = 0$. Taken from Ref. ³	19
2.6	Successive maxima of the asymptotic time evolution of $x(t)$ generated by Eq. (2.6) as function of the parameter a . Initial conditions are $\ddot{x} = \dot{x} = x = 0$. Taken from Ref. ³	20
3.1	a) Time evolution of the variables $x(t)$, $y(t)$, and $z(t)$ for the Linz-Sprott system Eqs.(3.1) with parameter $a = 0.6$. b) Corresponding chaotic attractor in the three-dimensional phase space. Integration was performed using the Runge-Kutta 4 (RK4) method with a time step $h = 0.1$ and $t = 100000$ iterations.	22
3.2	a) Time evolution of $x(t)$, $y(t)$, and $z(t)$ for the Sprott system with parameter $a = 0.553$. b) Corresponding periodic attractor in phase space. Integration was performed using the Runge-Kutta 4 (RK4) method with a time step $h = 0.1$ and $t = 100000$ iterations.	22
3.3	Representation of the global coupling mechanism in the system Eq. (3.2).	23
3.4	a) Time evolution of 10 variables $z_i(t)$ (color lines) for the globally coupled system Eqs. (3.2) over the first 2000 iterations. The thick black line represents the corresponding time evolution of z_{mean} . b) Time evolution of 10 variables $z_i(t)$ (color lines) and z_{mean} (black line) after transients. The trajectories overlap, indicating a collective synchronized state. Parameter values are $a = 0.553$, $\epsilon = 0.0001$, step $h = 0.1$, and number of iterations $t = 100000$. System size $N = 100$	24
3.5	Collective period attractor for the globally coupled system Eqs. (3.2), obtained by plotting the mean values x_{mean} , y_{mean} , and z_{mean} over an asymptotic time interval. This corresponds to a synchronized collective periodic orbit for the system. Parameter values are $a = 0.553$, time step $h = 0.1$	25
3.6	Time-averaged standard deviation σ as a function of the coupling parameter ϵ in the globally coupled network Eqs. (3.2) for fixed $a = 0.533$, $N = 100$. Values $\sigma \rightarrow 0$ indicate synchronization.	26

3.7 a) Representation of local dynamics in a network with $M = 2$ for a randomly selected agent i . Ring network with local couplings and periodic boundary conditions. Each element is coupled to M neighbors on each side. Here $M = 2$. b) Representation of the globally coupled dynamics with $M = \frac{N}{2}$ for a randomly selected agent i 27

3.8 a) Time evolution of the variables z_i for three elements (color lines) and the mean z_{mean} (black line) in a locally coupled system Eq. (3.5) with $a = 0.553$, coupling strength $\epsilon = 0.004$, $M = 1$ (one neighbor on each side), $N = 100$. b) Time evolution of the time-averaged standard deviation, σ for the locally coupled system Eq. (3.5) and same parameters as (a). 28

3.9 Time evolution of the standard deviation σ in the locally coupled system Eq. (3.5) with $a = 0.553$, coupling strength $\epsilon = 0.004$, $N = 100$ and $M = N/2$ (global limit). 29

3.10 Average standard deviation σ as a function of the coupling range M in the locally coupled network Eq. (3.5). Fixed parameters are $a = 0.553$, $\epsilon = 0.0038$, size $N = 100$. The globally coupled limit corresponds to $M = 50$ 30

3.11 Average standard deviation σ as a function of the normalized coupling range $M_{\text{normalized}}$ and the coupling strength ϵ for the locally coupled network Eq. (3.5). Color code is shown on the right bar. Darker regions represent areas of low dispersion or synchronization, while bright regions indicate higher dispersion. This visualization provides insights into the combined effects of local interaction range and coupling strength on the system's dynamics. Fixed parameters are $a = 0.553$, size $N = 100$ 31

Chapter 1

Introduction

The investigation of collective behaviors in networks of interacting dynamical elements has fundamental implications for understanding universal properties arising in complex systems. In this sense, of special interest is the phenomenon of nontrivial collective behavior, which consists of the coexistence of dissimilar time evolution of macroscopic quantities and microscopic variables in a system^{4,5}. This behavior manifests itself in two ways. On the one hand, it has been discovered the emergence of order in the temporal evolution of the dynamics of macroscopic quantities of a system of coupled chaotic elements. For example, the average of the states of the system can be periodic in time, while the evolution of the individual components is chaotic and desynchronized. This phenomenon has been widely studied⁶⁻⁹. On the other hand, this phenomenon has also been observed: spatiotemporal. This nontrivial behavior has been nominated collective chaos¹⁰⁻¹² and is one of the least understood emergent phenomena in complex systems.

The irregular or disordered collective behavior that emerges from coupled periodic elements can be classified into two types: (i) *Transient chaos*, which consists of a truly chaotic regime with a finite life time, and it is characterized by the coexistence of stable attractors and non-attractive chaotic sets (called repellers) in the phase space of a system. In this type of systems, a generic initial configuration produces a trajectory typically irregular until it abruptly collapses into a non-chaotic attractor¹³⁻¹⁵. (ii) *Collective stable chaos*; that constitutes an irregular behavior that cannot be described by the presence of repellers in the space phase of the system, resulting in the divergence of nearby trajectories. In this type of systems, the time spent during the transient regime can scale exponentially with the size of the system, and the asymptotic stable attractor cannot be reached in practical terms for large enough systems^{1,10,16-19}.

Transient spatiotemporal chaos has been studied in reaction-diffusion systems, such as Gray-Scott's equations^{13-15,20}, where it has been found that the spatial boundary conditions can induce the collapse of transient chaos towards a fixed point. On the other hand, long transients appear in networks of model neurons when the number of connections per neuron is small²¹.

In the case of stable collective chaos, the transient collective behavior, which is usually considered irrelevant, becomes statistically stationary and chaotic. The behavior of the system in the transient regime could not be distinguished from a typical chaotic behavior. There exist supertransients in these systems, since the chaotic collective behavior results, even for a moderately small system size, the only practically observable behavior. This phenomenon was first reported in a network of coupled chaotic maps^{1,16}. In these works, the authors studied models of coupled map network showing that, for a network of moderate size of 128 elements and, taking into account the speed and precision of the computer, they obtained that the characteristic time of the supertransient regime can be of the order of 10^{64} years. As a reference, consider that the current estimated age of our Universe, corresponds to 13.7×10^9 years, based on the recent data and analysis of the WMAP satellite (*Wilkinson Microwave Anisotropy Probe*)²². This result has a profound impact on some physical phenomena that have not yet been fully understood, as in the case of turbulence or the observation of aperiodic behaviors in complex systems, since such behaviors could correspond, from a strictly mathematical point of view, to a transitory state. From a practical point of view, we never will observe the regular asymptotic behavior, and what is truly stationary

will in fact be the supertransient regime of collective chaos^{1,11,12,17,18}.

The presence of local couplings between the elements in a network seems to be a common ingredient in all systems where collective chaos has been observed¹⁹. Thus, the role of the topology of the network on the occurrence of this collective phenomenon has not been fully investigated.

1.1 Research problem

In this Thesis we shall explore the influence of the network connectivity on the emergence of collective spatiotemporal chaos. In particular, we shall investigate this phenomenon in globally coupled networks where the coupling between the elements is all-to-all. Since most work on collective chaos have been carried out in coupled map networks where time is discrete, we shall study time-continuous dynamics on networks in order to explore the generality of the phenomenon. In this regard, we shall employ an elementary time-continuous chaotic system as local dynamics in order to search for minimal conditions for the emergence or collapse of collective spatiotemporal chaos.

1.2 Objectives

1.2.1 General objective

To explore the effect of the network connectivity on the emergence of spatiotemporal collective chaos in continuous-time dynamical networks.

1.2.2 Specific objectives

1. To investigate the occurrence of spatiotemporal collective chaos in globally coupled networks.
2. To employ time-continuous dynamical systems as the coupled units in networks exhibiting spatiotemporal collective chaos.
3. To investigate the role of the range of interaction on the emergence of spatiotemporal collective chaos in dynamical networks.

Chapter 2

Theoretical framework

2.1 Supertransient chaos

Chaos occurs commonly in nonlinear spatially extended dynamical systems that can be typically described by partial differential equations, coupled ordinary differential equations, coupled map networks, or cellular automata. In systems described by partial differential equations, the state variables, space, and time, are all continuous. Coupled differential equations possess continuous states, discrete space corresponding to the coupling network, and continuous time. Coupled map networks are spatiotemporal dynamical systems where space and time are discrete, but the state variables are continuous. Cellular automata are characterized by having discrete states, discrete space and discrete time.

If the patterns generated by such a system are ordered in space, we speak of a pattern formation process. If the patterns are spatially irregular, we speak of spatiotemporal chaos.

In many dissipative spatiotemporal systems, chaos appears as a transient phenomenon. The reason is that spatial coupling is typically diffusive, so that neighboring sites tend to behave similarly or synchronize. The asymptotic attractors are often periodic in time or stationary. It is the approach towards these attractors which is chaotic. In this sense, spatiotemporal chaos often collapses after some time, and a regular behavior then takes over. Thus, we are naturally interested in the scaling law of the transient lifetime, or the escape rate (the inverse of the lifetime), with the system size. If the lifetime increases rapidly with the system size, we speak of supertransients. An important physical example of supertransients is turbulence in fluid flows. Here the well-known stationary laminar solution is the only asymptotic attractor, and the observed turbulent behavior appears to be a kind of transient chaos.

In large size systems exhibiting supertransients, it is not possible to determine whether the observed “turbulence” is transient unless an asymptotic time regime is reached. If the transient time is much longer than any physically realizable time, the system is effectively “turbulent,” regardless of the nature of the asymptotic attractor. In this case, the transients hide the real attractor, and pose a fundamental difficulty for observing the asymptotic state of the system. In this sense, attractors are irrelevant to “turbulence”¹⁶. Supertransients are considered the most surprising applications of the concept of transient chaos to spatially extended dynamical systems¹⁹.

The first observation of supertransient behavior in spatiotemporal dynamical systems was reported by Crutchfield and Kaneko¹⁶ in a model of coupled map ring lattice with nearest-neighbor coupling, where the local maps possess a stable periodic orbit. A simpler system was employed by Kaneko¹ to show this phenomenon in the following one-dimensional coupled map lattice,

$$x_{n+1}(i) = (1 - \epsilon)f(x_n(i)) + \frac{\epsilon}{2} [f(x_n(i+1)) + f(x_n(i-1))]. \quad (2.1)$$

where $i = 1, 2, \dots, N$; N is the size of the system, $x_n(i)$ is the state of the i th element at discrete time $n = 0, 1, 2, \dots$, ϵ is a parameter expressing the strength of the coupling, and the function $f(x_n(i)) = 1 - ax_n(i)^2$ describes the local dynamics that depends on the parameter a . Periodic boundary conditions are assumed in the system Eqs. (2.1); that is the lattice

corresponds to a one-dimensional ring. The coupling scheme in Eqs. (2.1) is called diffusive, because it corresponds to the discrete form of the Laplacian operator in a diffusion equation.

For the parameter value $a = 1.752$ there exists a stable period-3 orbit $x_1^* \rightarrow x_2^* \rightarrow x_3^*$ in the local map, such that $f^{(3)}(x_1^*) = x_1^*, f^{(3)}(x_2^*) = x_2^*, f^{(3)}(x_3^*) = x_3^*$. The synchronized, collective period-3 state is stable for values of the coupling $\epsilon > 10^{-3}$. However, if the size of the system is sufficiently large, this synchronized state is never reached from arbitrarily chosen initial conditions. Figure 2.1 shows the spatiotemporal pattern resulting in the system Eqs. (2.1) for parameter values $a = 1.752$ and $\epsilon = 1.05 \times 10^{-3}$, for which a stable synchronized state exists. We can see that for large times, the system has not yet settled into the synchronized period-3 state.

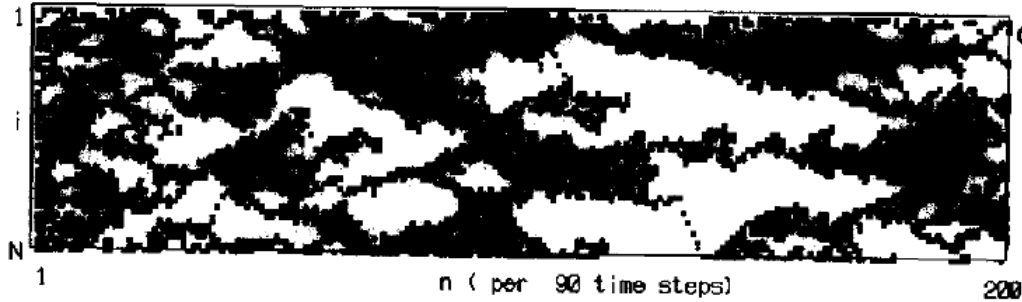


Figure 2.1: States $x_n(i)$ of $N = 50$ maps as functions of discrete time n for the system Eqs. (2.1) with parameter values $a = 1.752$ and $\epsilon = 1.05 \times 10^{-3}$, plotted every 90 time steps. Color code is as follows: if $|x_n(i + 1) + x_n(i)| < 0.3$ the i th site is white, otherwise it is black. Taken from Ref.¹

Kaneko¹ found that the average transient time T to reach the synchronized, spatially homogeneous state, increases exponentially with the system size N , for coupling parameter values $\epsilon > 10^{-3}$, as Fig. 2.2 shows. That is, $T \propto e^N$.

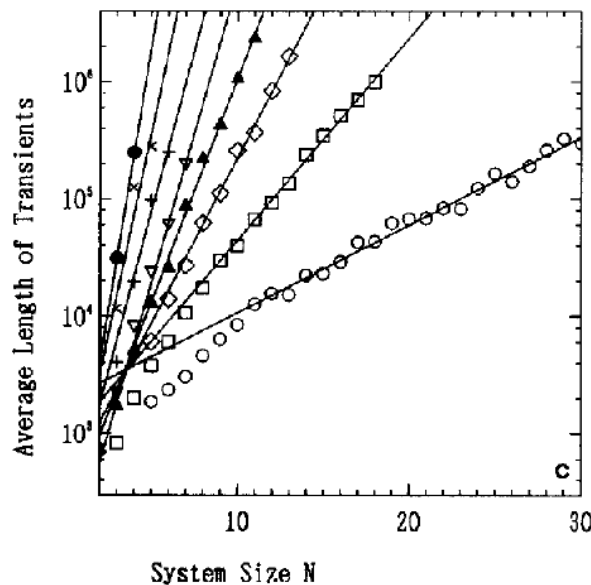


Figure 2.2: Semi-log plots of the average transient times T versus the logarithm of the system size N of the system Eqs. (2.1), for different values of the coupling strength ϵ . Fixed parameter $a = 1.752$. The symbols indicate different values, ranging from $\epsilon = 0.0011$ (open circles) to $\epsilon = 0.005$ (full black circles). Taken from Ref.¹

Supertransient behavior with lifetimes scaling exponentially with the system size have been found in a variety of systems possessing local or near-neighbor couplings, other than coupled map networks, such as the Kuramoto–Shivashinsky

equation²³, Complex Ginzburg–Landau equation²⁴, reaction–diffusion systems¹³, turbulent shear flow²⁵.

2.2 Collective stable chaos

In certain systems, supertransients are characterized by the a negative maximum Lyapunov exponent even during the transient behavior, resulting in the divergence of nearby trajectories. This phenomenon has been denoted as stable chaos¹⁰. Stable chaos constitutes a non-trivial collective behavior, where an irregular unpredictable behavior emerges in the macroscopic variables of a system emerges from a regular local behavior of its interacting elements.

A local map possessing minimal ingredients for displaying stable collective chaos in a coupled map lattice system Eqs. (2.1) is the following¹⁰

$$f(x) = \begin{cases} bx, & 0 < x < 1/b, \\ a + c(x - 1/b), & 1/b < x < 1, \end{cases} \quad (2.2)$$

where $x \in (0, 1)$ and the parameters a, b are chosen so that the map dynamics yields a superstable period–3 orbit, corresponding to the points $x_1^* = a \rightarrow x_2^* = ab \rightarrow x_3^* = ab^2$. A superstable orbit has a Lyapunov exponent equal to $-\infty$. It can be achieved with parameter values $a = 0.1, b = 2.5$ and $c = 0$. Figure 2.3 shows the function Eq. 2.2 for these values of parameters and the bifurcation diagram of the map $x_{n+1} = f(x_n)$ as a function of b .

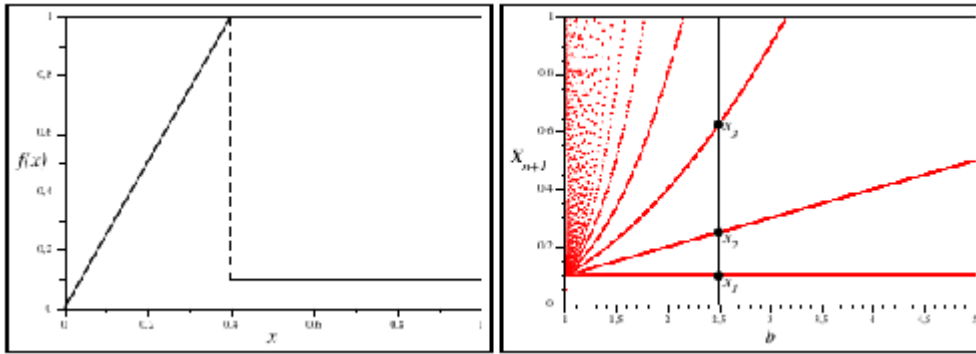


Figure 2.3: Left: Local map Eq. 2.2 with $a = 0.1, b = 2.5$ and $c = 0$. Right: Bifurcation diagram of map Eq. 2.2 as a function of b for fixed parameter values $a = 0.1$ and $c = 0$. The values of the period–3 superstable orbit are indicated by black dots.

The stability of the superstable periodic orbit of the local map (2.2) implies the stability of the synchronized orbit system Eqs. (2.1), whose maximum Lyapunov exponent becomes negative for all values of ϵ . As a consequence, the long time evolution of the coupled system Eqs. (2.1) is constrained to its periodic attractor.

Following Ref.², the collective behavior of the coupled map system Eqs. (2.1) can be characterized by the mean field of the system, defined as

$$H_t = \frac{1}{N} \sum_{j=1}^N x_n(j). \quad (2.3)$$

Similarly, the synchronization of the elements in the system Eqs. (2.1) can be measured by the asymptotic time average $\langle \sigma \rangle$ of the standard deviation σ_t at time $t = n$ of the distribution of the map state variables $x_n(i)$, given by

$$\sigma_t = \left[\frac{1}{N} \sum_{i=1}^N (x_n(i))^2 - H_n^2 \right]^{1/2}. \quad (2.4)$$

A synchronized state corresponds to $\langle \sigma \rangle = 0$. In practice, the criterion $\langle \sigma \rangle \leq 10^{-7}$ is employed for synchronization. In the present case, the system Eqs. (2.1) can synchronize in the superstable period–3 orbit of the local map Eq. 2.2.

Figure 2.4 shows the quantities H_t and the average dispersion $\langle\sigma\rangle$ as functions of the coupling parameter ϵ for the system of maps Eqs. (2.1). Note that H_t does not reach a collective period-3 motion and the system never synchronizes ($\langle\sigma\rangle = 0$) over a range of ϵ .

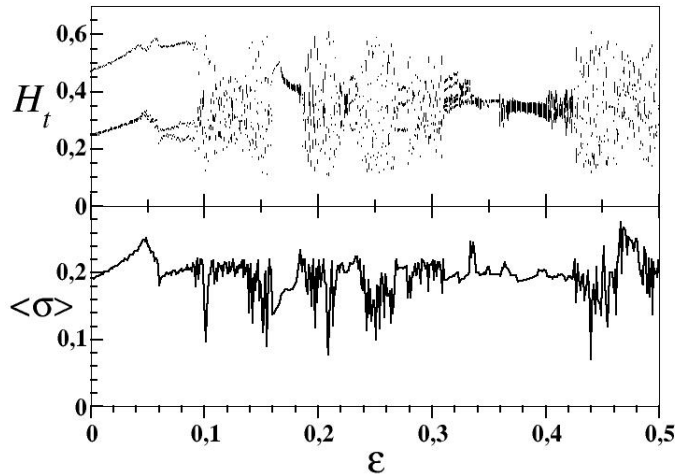


Figure 2.4: Bifurcation diagram of the mean field H_t and the average dispersion $\langle\sigma\rangle$ as functions of ϵ for the system Eqs. (2.1) with size $N = 10^3$. For each value of ϵ 10^3 values of H_t are plotted, after discarding 10^4 transients. The quantity $\langle\sigma\rangle$ is calculated as the average of 10^3 values of σ_t , after discarding 10^4 transients. Taken from Ref.².

In all the systems where collective chaos has been observed, the presence of local couplings between the elements seems to be a common condition¹⁹. In this Thesis we shall explore the influence of the topology of connectivity between the elements on the emergence of collective spatiotemporal chaos. In particular, we shall investigate this phenomenon in globally coupled systems where the coupling between the elements is all-to-all.

Since most work on this phenomenon have been carried out in coupled map systems, we shall study collective chaos in time-continuous dynamics. In this regard, we shall employ an elementary time-continuous chaotic system as local dynamics in order to search for minimal conditions for the emergence of collective spatiotemporal chaos.

2.3 Globally Coupled Systems

Globally coupled dynamical networks, where each element interacts with each other in the system, constitute paradigmatic models for the current research of complex systems that possess global interactions²⁶. A global interaction occurs when all the elements in the system are subject to the same influence or share the same information. Many physical, chemical, biological, social, and economic systems are subject to global interactions. Global interactions can provide useful descriptions in networks possessing highly interconnected elements or long-range interactions. The origin of a global interaction can be either external, as in a forcing field; or autonomous, such as a mean field or a feedback coupling function that depends on the elements of the system²⁷. Global interactions appear, for example, in parallel electric circuits, coupled oscillators^{28,29}, charge density waves³⁰, Josephson junction arrays³¹, multimode lasers³², neural networks, evolution models, ecological systems³³, social networks³⁴, economic exchange³⁵, mass media influence³⁶⁻³⁸, and cultural globalization³⁹. Diverse collective behaviors have been observed experimentally in globally coupled oscillators, such as complete and generalized chaos synchronization, dynamical clustering, nontrivial collective behavior, chaotic itinerancy, quorum sensing, and chimera states⁴⁰⁻⁴⁵.

In this Thesis we shall investigate the phenomenon of spatiotemporal collective chaos in systems possessing global interactions.

2.4 Elementary chaotic flow

Poincarè-Bendixson theorem prevents the existence of chaos in two-dimensional dynamical system, since the only possible asymptotic solutions in this case are fixed points or limit cycles (i. e. periodic orbits). Thus, chaotic behavior requires a phase space of dimension 3 at least. The other necessary condition is the presence of non-linearity in the equations that describe the dynamics.

In 1999, Linz and Sprott reported the simplest known 3-dimensional continuous-time dynamical system exhibiting chaos³,

$$\ddot{x} + a\dot{x} + \dot{x} - |x| + 1 = 0, \quad (2.5)$$

where a is a real parameter. This a differential equation of third order which can be written as a system of three differential equations of first order as follows,

$$\begin{aligned} \dot{x} &= y, \\ \dot{y} &= z, \\ \dot{z} &= -az - y + |x| - 1. \end{aligned} \quad (2.6)$$

The system has 3 dimensions in phase space and possess only one parameter. It has only one non-linearity given by the modulus of x , which is the simplest nonlinear function one may consider. Figure 2.5 shows an image of the strange attractor arising in the Linz-Sprott system Eqs. (2.6).

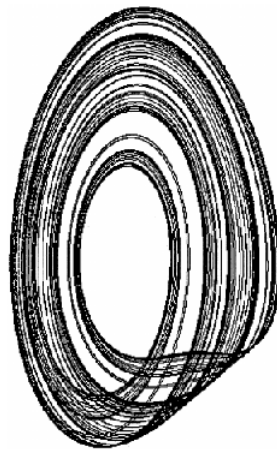


Figure 2.5: View of the chaotic attractor of the system Eqs. (2.6) for the parameter value $a = 0.6$. Initial conditions are $\ddot{x} = \dot{x} = x = 0$. Taken from Ref.³.

Figure 2.5 shows a bifurcation diagram of the solutions of the Linz-Sprott system as a function of the parameter a .

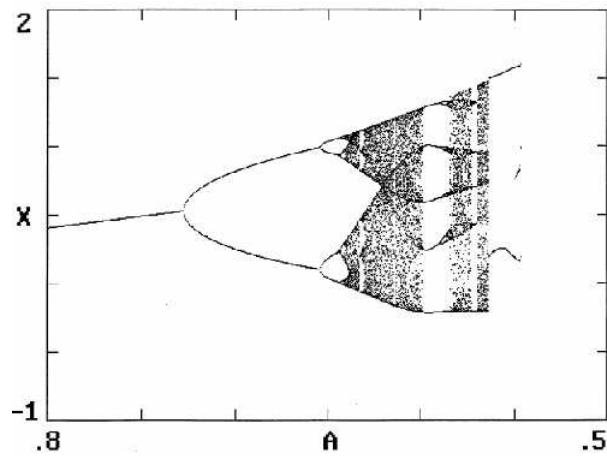


Figure 2.6: Successive maxima of the asymptotic time evolution of $x(t)$ generated by Eq. (2.6) as function of the parameter a . Initial conditions are $\ddot{x} = \dot{x} = x = 0$. Taken from Ref. ³.

In next chapter, we shall use a network of coupled Linz-Sprott systems to study the emergence of collective spatiotemporal chaos in continuous-time systems.

Chapter 3

Spatiotemporal chaos in continuous-time dynamical networks

3.1 Numerical solution of Linz-Sprott's Equations

In this chapter, we present the main results of our work. We investigate the role of the connectivity of the network on the emergence of collective spatiotemporal chaos in systems possessing continuous-time dynamics. Since we are searching for the minimal conditions for the occurrence of this collective phenomenon, we shall employ, as local continuous-time dynamics, the Linz-Sprott equations³.

To validate our numerical approach, it is essential to first reproduce the behavior of the Linz-Sprott equations. This equation is notably known as the simplest chaotic system with continuous time⁴. Successful reproduction of the solutions of the Linz-Sprott equation affirms the accuracy of our numerical approach to be used in subsequent calculations of our study.

The Linz-Sprott system is represented by the following three coupled first order differential equations³

$$\begin{aligned}\dot{x} &= y, \\ \dot{y} &= z, \\ \dot{z} &= -az - y + |x| - 1.\end{aligned}\tag{3.1}$$

The Linz-Sprot system is three-dimensional in phase space and possess only one parameter. It has only one non-linearity given by the modulus of x , which is the simplest nonlinear function one may consider. In comparison, the famous Lorenz equations, where chaos was discovered, have two non-linear terms of quadratic order.

In this form, we can implement a Four-order Runge-Kutta method to numerically integrate the system Eqs.(3.1).

We examine the behavior of the Linz-Sprott system for two distinct parameter settings leading to chaotic and to periodic solutions. Figure 3.1 shows the solutions of the Linz-Sprott system for the parameter value $a = 0.6$, for which chaotic behavior takes place.

Figure 3.2 shows the solutions of the Linz-Sprott system for the parameter value $a = 0.553$, which, according to Fig. (2.6), should yield a periodic orbit. In fact, we observe periodic behavior in the time evolution of $x(t)$, $y(t)$, and $z(t)$. The maxima of these variables display a period-3 orbit.

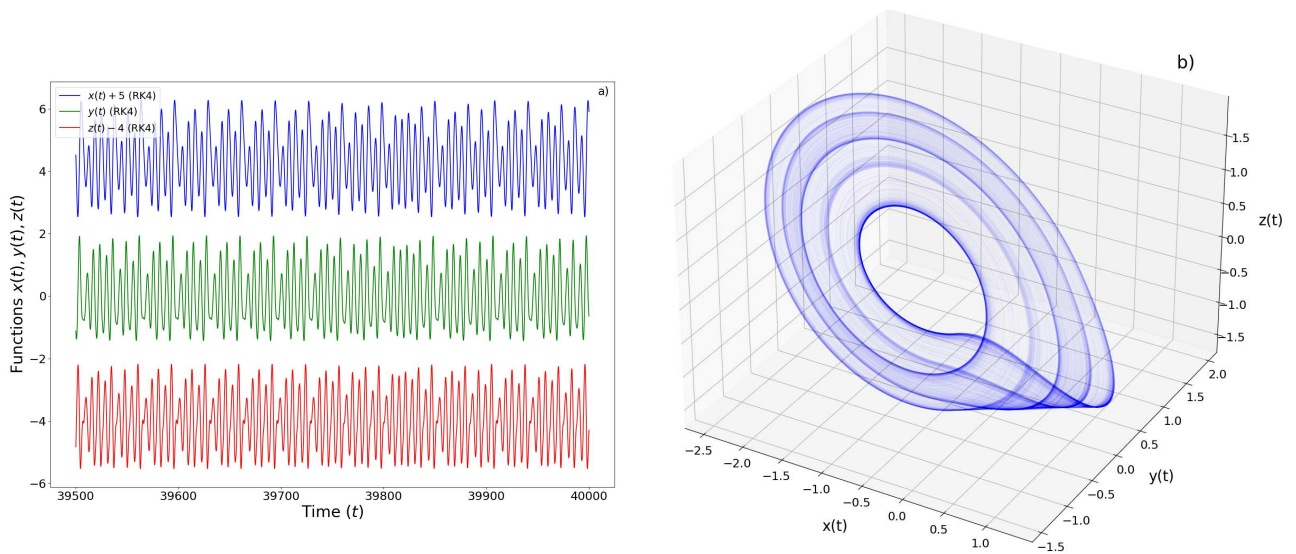


Figure 3.1: a) Time evolution of the variables $x(t)$, $y(t)$, and $z(t)$ for the Linz-Sprott system Eqs.(3.1) with parameter $a = 0.6$. b) Corresponding chaotic attractor in the three-dimensional phase space. Integration was performed using the Runge-Kutta 4 (RK4) method with a time step $h = 0.1$ and $t = 100000$ iterations.

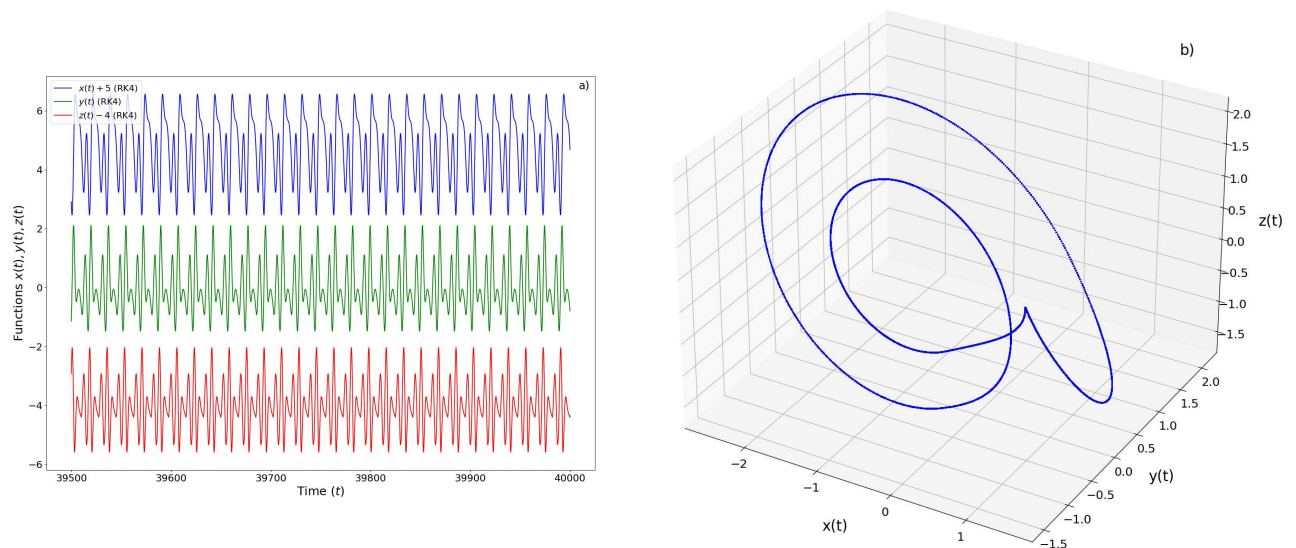


Figure 3.2: a) Time evolution of $x(t)$, $y(t)$, and $z(t)$ for the Sprott system with parameter $a = 0.553$. b) Corresponding periodic attractor in phase space. Integration was performed using the Runge-Kutta 4 (RK4) method with a time step $h = 0.1$ and $t = 100000$ iterations.

3.2 Globally coupled network

Consider a set of N Sprott systems, each described by 3 state variables x_i, y_i, z_i , where $i = 1, 2, \dots, N$. To introduce a global interaction, we incorporate a term in the third equation, which essentially captures the average behavior of the set of N systems. We consider a globally coupled system described as

$$\begin{aligned} \dot{x}_i &= y_i, \\ \dot{y}_i &= z_i, \\ \dot{z}_i &= (1 - \epsilon)(-az_i - y_i + |x_i| - 1) + \epsilon z_{\text{mean}}, \end{aligned} \tag{3.2}$$

where ϵ is the coupling coefficient representing the strength of the interaction between the systems. The term z_{mean} represents the mean of all the variables z_i values in the system, defined as

$$z_{\text{mean}}(t) = \frac{1}{N} \sum_{j=1}^N z_j(t). \tag{3.3}$$

The factor $(1 - \epsilon)$ affecting the local variable z_i is typical of diffusive coupling. It also contributes to compensate the additional term and to keep the orbits bounded in phase space. The globally coupled network Eq. (3.2) consists of $3N$ coupled first order differential equations.

Through the modified third equation, each system is influenced by the average behavior of all systems, then sharing a global interaction. Figure 3.3 provides a visual representation of this global coupling mechanism, illustrating how each individual system is influenced by the average behavior of all systems, through the term z_{mean} .

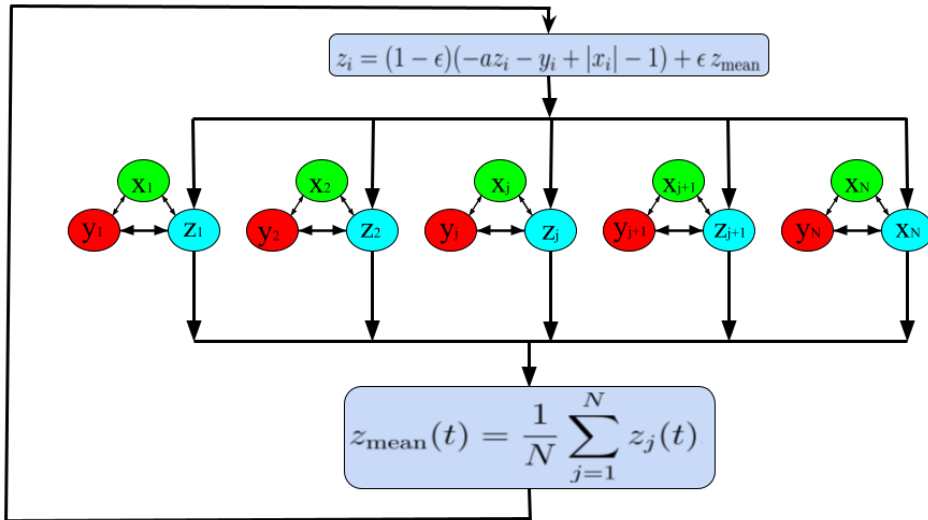


Figure 3.3: Representation of the global coupling mechanism in the system Eq. (3.2).

3.2.1 Collective synchronization of periodic orbits

The introduction of even minimal coupling can induce behaviors that remain elusive in isolated systems. Thus, we search for coupling parameter values promoting synchronization that would represent the collapse of supertransient spatiotemporal chaos.

Figure (3.4) shows the time evolution of a subset of randomly chosen 10 Linz-Sprott systems in the globally coupled network Eq. (3.2) with size $N = 100$. The local parameters of all elements are fixed at the value $a = 0.553$ for which a stable periodic orbit exists in a single Linz-Sprott system. Note that, after some transients, the globally coupled system synchronizes to this periodic orbit, in contrast to the supertransient behavior observed in locally coupled networks. Synchronization here is characterized by the time evolution $z_{\text{mean}}(t) = z_i(t), \forall i$.

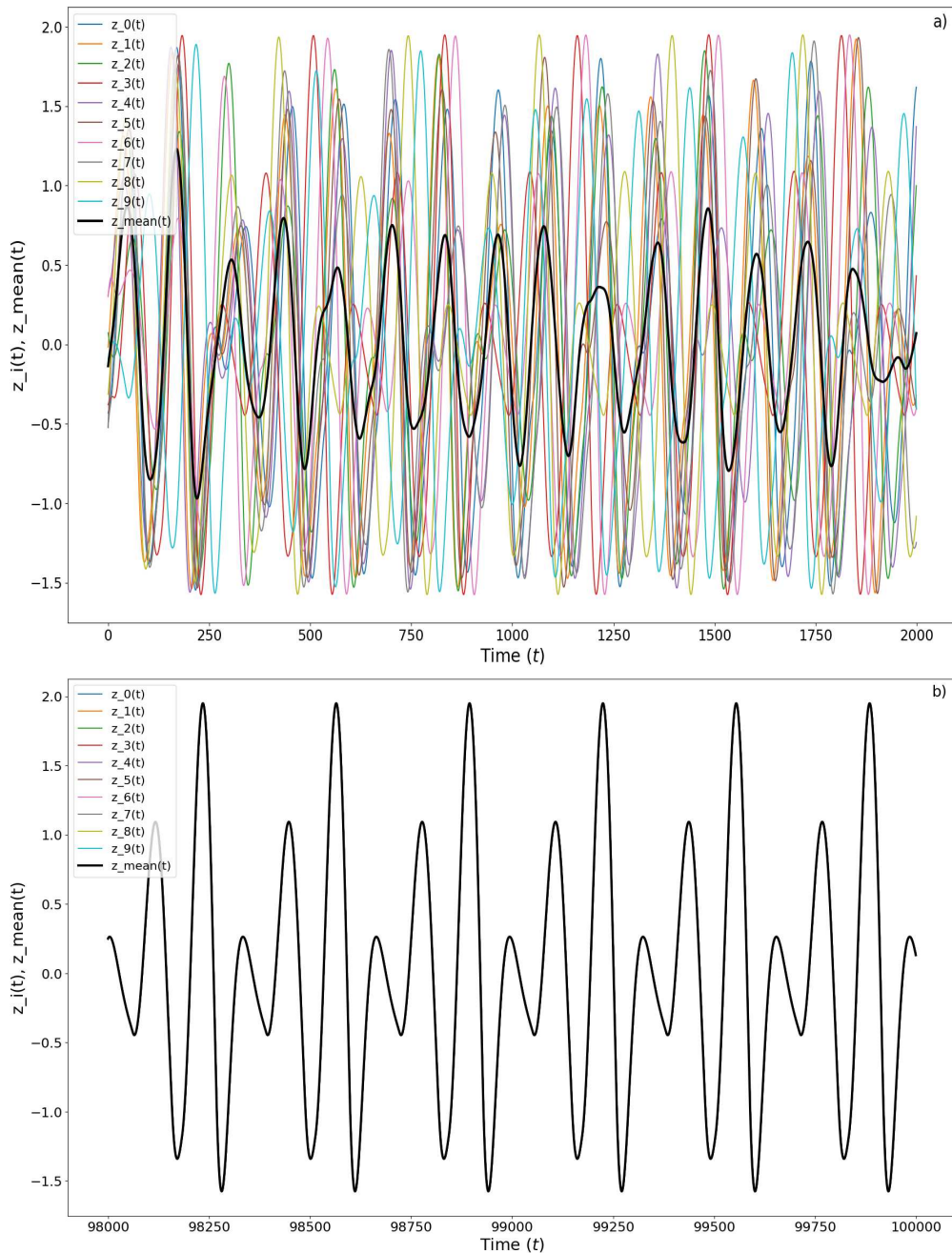


Figure 3.4: a) Time evolution of 10 variables $z_i(t)$ (color lines) for the globally coupled system Eqs. (3.2) over the first 2000 iterations. The thick black line represents the corresponding time evolution of z_{mean} . b) Time evolution of 10 variables $z_i(t)$ (color lines) and z_{mean} (black line) after transients. The trajectories overlap, indicating a collective synchronized state. Parameter values are $a = 0.553$, $\epsilon = 0.0001$, step $h = 0.1$, and number of iterations $t = 100000$. System size $N = 100$.

In Fig. 3.4a, which portrays the evolution of 10 $z_i(t)$ variables across the first 2000 iterations, it becomes apparent that each of the 10 systems, endowed with distinct initial conditions, unfolds its own individual periodic trajectory. This indicates a difference among these trajectories, underscoring the absence of synchronization during the early iterations.

On the other hand, transitioning to a longer temporal scale, Figure 3.4b shows the dynamics for the last 2000 iterations. A stark difference with the initial stages is observed. The trajectories, instead of diverging, seem to converge, overlapping in phase and amplitude. This synchronization is indicative of the systems having attained a common state, with each

equation oscillating coherently with the others. The observation of this collective synchronized state, achieved in the latter iterations, reveals that the chosen coupling value, $\epsilon = 0.0001$, resides within the threshold necessary to facilitate synchronization in the globally coupled network Eq. (3.2).

To visualize the emergent synchronization in the globally coupled network, we present Figure 3.5. This figure shows the trajectory of the mean variables in the phase space constructed using the mean values x_{mean} , y_{mean} , and z_{mean} over an extended time span. Clearly discernible within this representation is a periodic—3 trajectory. Such an evident periodicity in the average values indicates that the synchronization within the system has indeed been achieved and that any supertransient behavior has disappeared in a finite time.

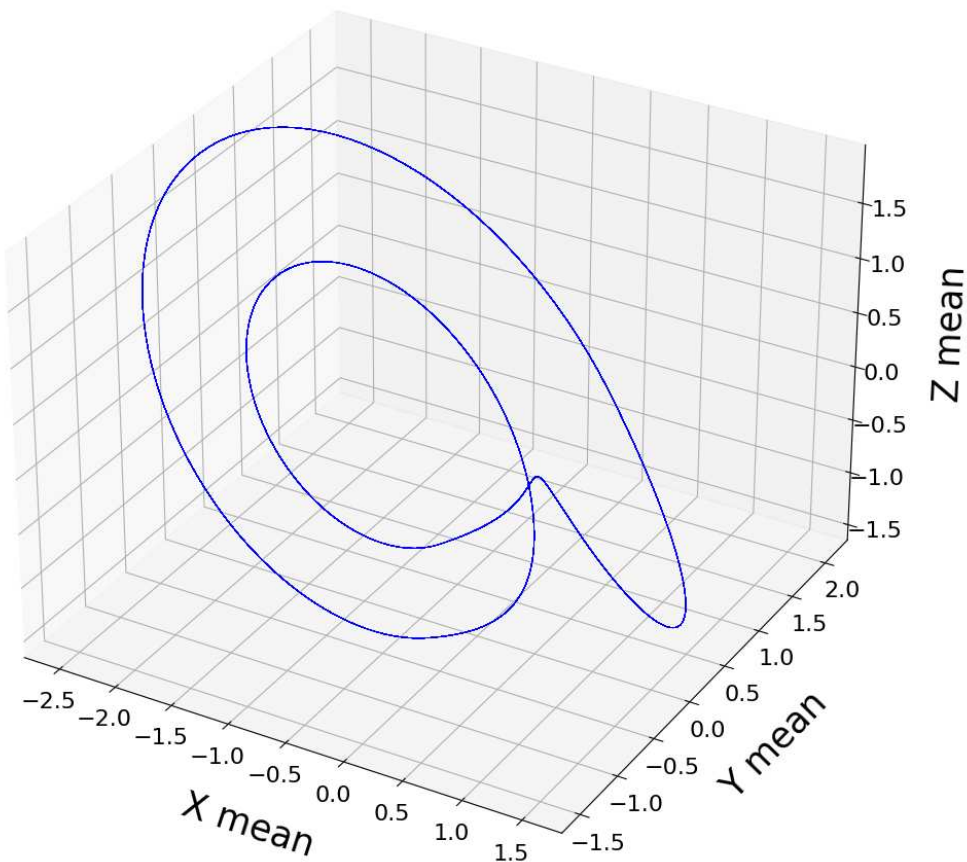


Figure 3.5: Collective period attractor for the globally coupled system Eqs. (3.2), obtained by plotting the mean values x_{mean} , y_{mean} , and z_{mean} over an asymptotic time interval. This corresponds to a synchronized collective periodic orbit for the system. Parameter values are $a = 0.553$, time step $h = 0.1$.

3.2.2 Characterizing synchronization.

Determining the appropriate values of ϵ was essential to comprehend how minimal coupling could lead to synchronization and the collapse of collective chaos. With this in mind, we set out to identify the coupling values for which the globally coupled network Eq. (3.2) synchronizes.

To ascertain synchronization, we employ the standard deviation, represented as σ . The standard deviation quantifies the dispersion or variation in a dataset. For a set of N numbers z^1, z^2, \dots, z^N , the instantaneous standard deviation, $\sigma(t)$,

of the z_i variables is determined by:

$$\sigma(t) = \sqrt{\frac{1}{N} \sum_{j=1}^N [z_j(t) - z_{\text{mean}}(t)]^2} \quad (3.4)$$

For the purpose of our analysis, it is important to note that we compute the standard deviation solely for the z_i variables, similar to our approach with global coupling. With this understanding, we observe the following results.

Figure 3.6 displays the relationship between the time-averaged standard deviation σ and the coupling parameter ϵ for the globally coupled network Eqs. (3.2). Here, the fixed parameters are $a = 0.53$ and $N = 100$. An observation of values $\sigma \rightarrow 0$ indicates the emergence of synchronization among the systems.

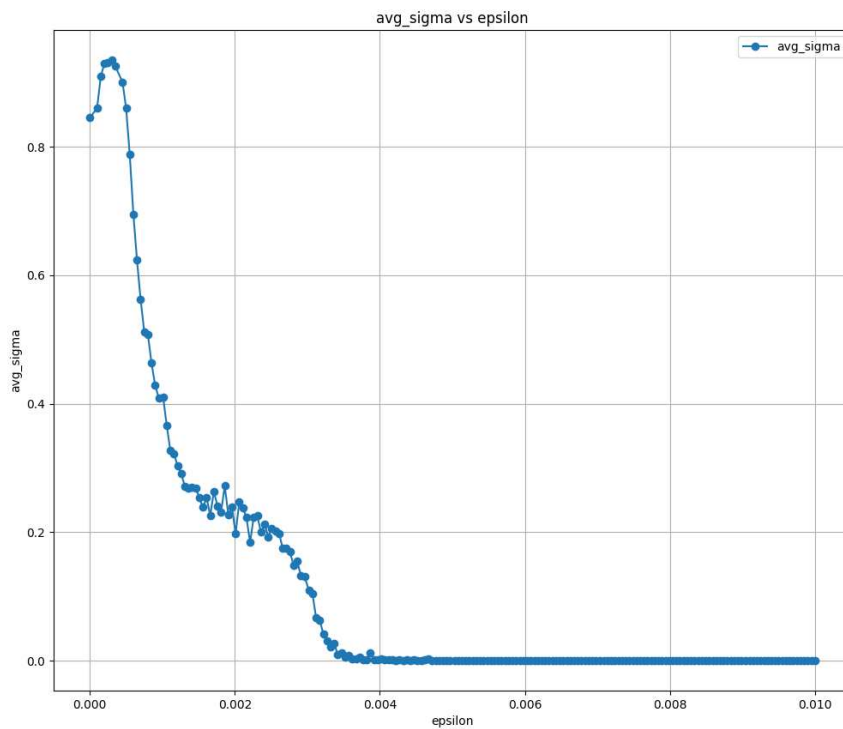


Figure 3.6: Time-averaged standard deviation σ as a function of the coupling parameter ϵ in the globally coupled network Eqs. (3.2) for fixed $a = 0.533$, $N = 100$. Values $\sigma \rightarrow 0$ indicate synchronization.

Figure 3.6 shows that there exists a critical threshold value of ϵ at which synchronization arises. Specifically, the figure indicates a critical value for synchronization at $\epsilon_c = 0.0037$. For values $\epsilon \geq \epsilon_c$, the network exhibits full synchronization, with the average standard deviation σ equating to zero.

This behavior underscores the significance of the coupling strength in globally coupled systems. The observed $\epsilon = 0.0037$ effectively serves as a bifurcation point where emergent synchronized behavior initiates. This is a testament to wherein even minimal interactions, when they surpass a certain critical threshold, can lead to the emergence of collective coherent behaviors in complex dynamical systems subject to global interactions.

The above results suggest that the phenomenon of supertransients is related to the presence of local interactions; it does not prevail in systems possessing global interactions. Thus, we shall investigate next the influence of the topology of the connectivity on the emergence of collective stable chaos.

3.3 Networks with varying range of interactions

After understanding the effect of global interactions in the phenomenon of collective chaos, we turn to study networks with local couplings. Here, unlike the global system where each part interacts with every other, in local coupling, they interact mainly with their neighborhood.

We consider a ring network where each element is coupled to its M neighbors on each side, as Fig. 3.7 a) illustrates.

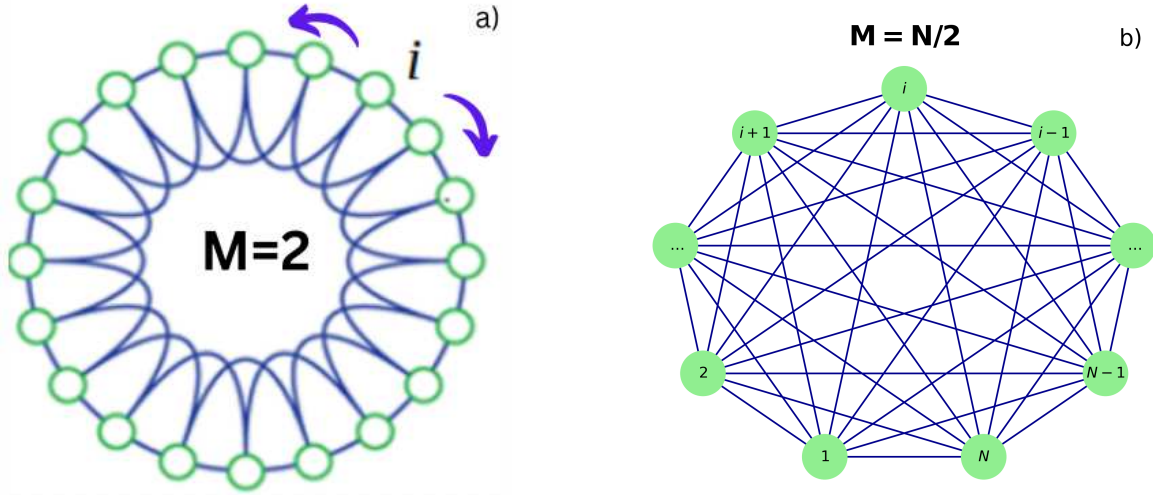


Figure 3.7: a) Representation of local dynamics in a network with $M = 2$ for a randomly selected agent i . Ring network with local couplings and periodic boundary conditions. Each element is coupled to M neighbors on each side. Here $M = 2$. b) Representation of the globally coupled dynamics with $M = \frac{N}{2}$ for a randomly selected agent i .

Then, we define the following equations for the locally coupled ring network of Linz-Sprott systems:

$$\begin{aligned}\dot{x}_i &= y_i, \\ \dot{y}_i &= z_i, \\ \dot{z}_i &= (1 - \epsilon)(-az_i - y_i + |x_i| - 1) + \epsilon Z_i\end{aligned}\tag{3.5}$$

with

$$Z_i = \frac{1}{2M + 1} \sum_{j=i-M}^{i+M} z_j\tag{3.6}$$

where ϵ is the coupling strength, $i = 1, 2, \dots, N$, and Z_i represents the interactions of the element i with its nearest M immediate neighbors on each side. The quantity Z_i computes the local average of the z_i variables in the vicinity of the i -th element.

We begin by analyzing the minimal local network configuration where $M = 1$. In this setup, each element has only two neighbors: one to its left and one to its right. This corresponds to the connectivity of the coupled map lattices where supertransient behavior was discovered.

Figure 3.8 a) shows the time evolution of the z_i variables of three randomly chosen elements and the quantity z_{mean} for the locally coupled ring network of Linz-Sprott systems Eq. (3.5). The local parameters are fixed at the value $a = 0.553$, for which the Linz-Sprott system is periodic. Figure 3.8b shows the time evolution of instantaneous standard deviation which does not fall to the value 0.

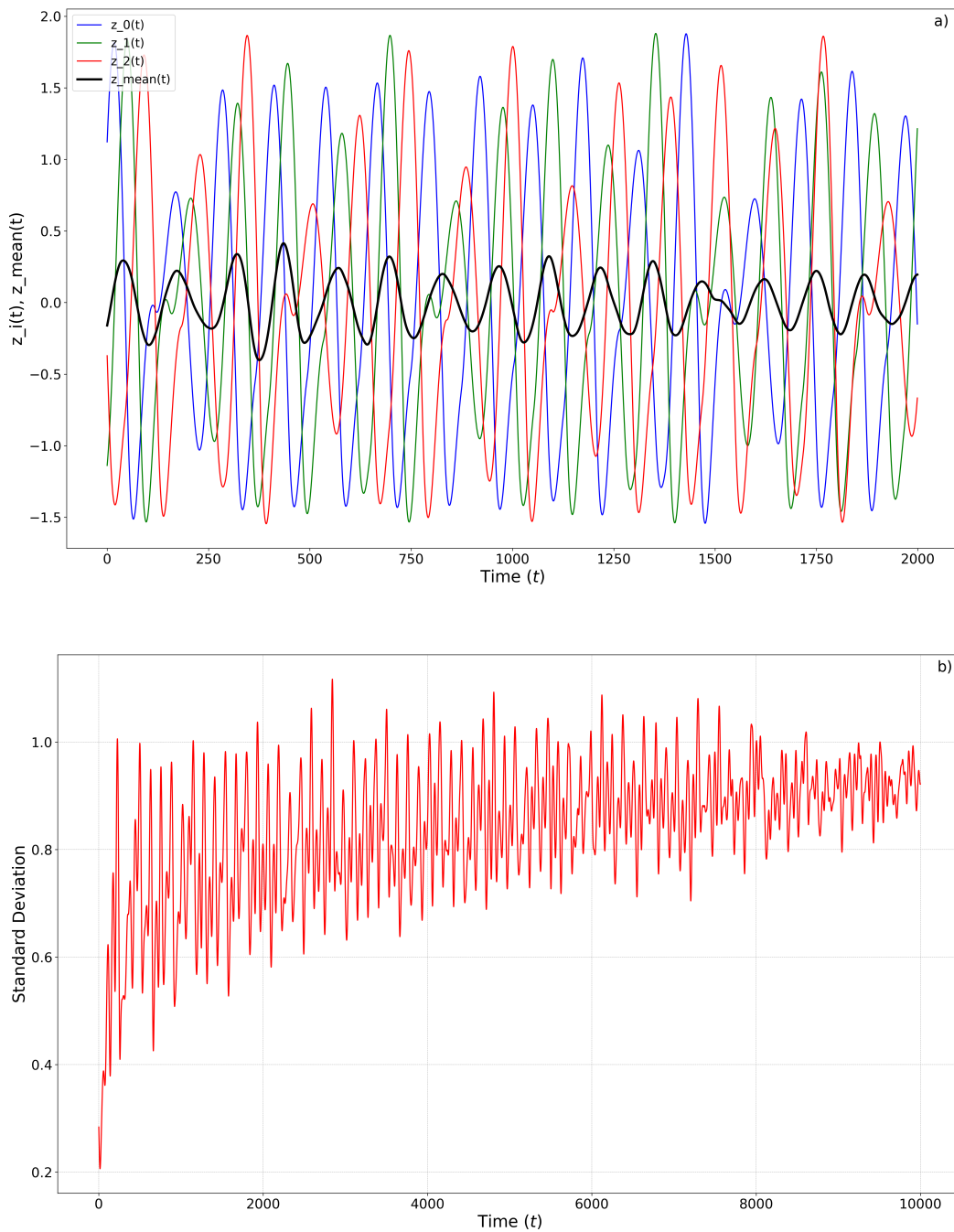


Figure 3.8: a) Time evolution of the variables z_i for three elements (color lines) and the mean z_{mean} (black line) in a locally coupled system Eq. (3.5) with $a = 0.553$, coupling strength $\epsilon = 0.004$, $M = 1$ (one neighbor on each side), $N = 100$. b) Time evolution of the time-averaged standard deviation, σ for the locally coupled system Eq. (3.5) and same parameters as (a).

Figure 3.8 reveals the lack of synchronization amongst the z_i values. The depicted trajectories of three distinct elements noticeably deviate from the overall mean trajectory z_{mean} , emphasizing the incoherent state of the network.

In the globally coupled network we have observed synchronization. To assess whether a similar behavior emerges in the locally coupled network in the limit of all-to-all interactions, we simulated it with the value $M = 50$.

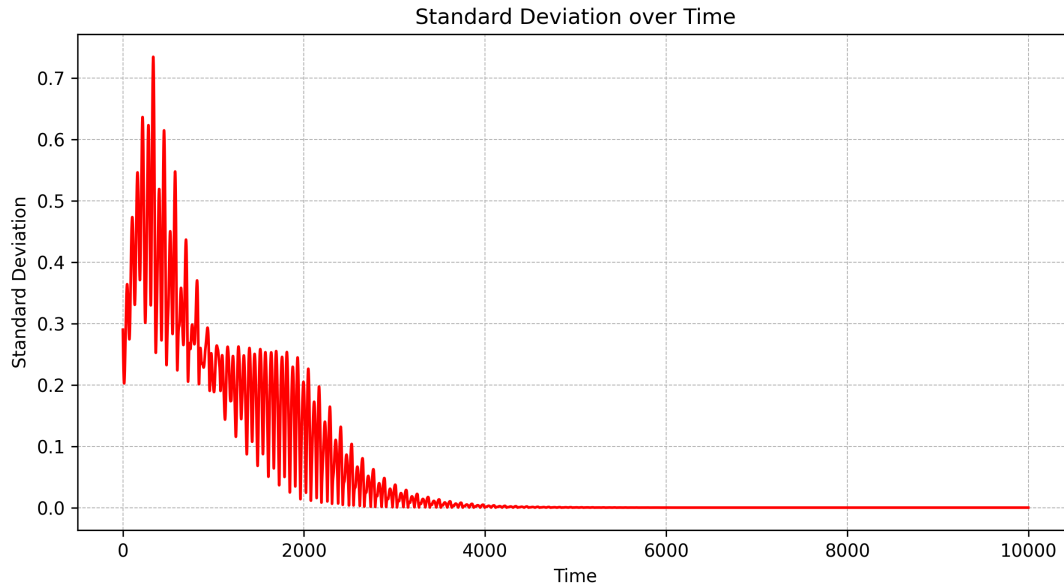


Figure 3.9: Time evolution of the standard deviation σ in the locally coupled system Eq. (3.5) with $a = 0.553$, coupling strength $\epsilon = 0.004$, $N = 100$ and $M = N/2$ (global limit).

Figure 3.9 shows the behavior of the locally coupled network Eq. (3.5) with $M = 50$. Specifically, the time evolution of the standard deviation σ steadily decreases towards zero, emphasizing the emergence of synchronization.

Building on these observations, we conduct a more in-depth analysis. It's essential to underscore that throughout this examination, all parameters known to induce synchronization are held constant. The only variable we adjust is the number of neighbors, M , to discern the influence of the range of interaction on the standard deviation σ , and therefore on the collapse of the spatiotemporal chaos.

This motivated us to investigate the relationship between the range of the interactions M and the standard deviation σ .

Figure 3.10 shows the average standard deviation σ as a function of the coupling range M in the locally coupled network Eq. (3.5). This plot serves as an indicator of the minimum number of neighbors or coupled equations required to achieve synchronization. From the figure, it is evident that approximately $M = 20$ is the threshold for the number of equations that need to be coupled for the given parameter value of ϵ .

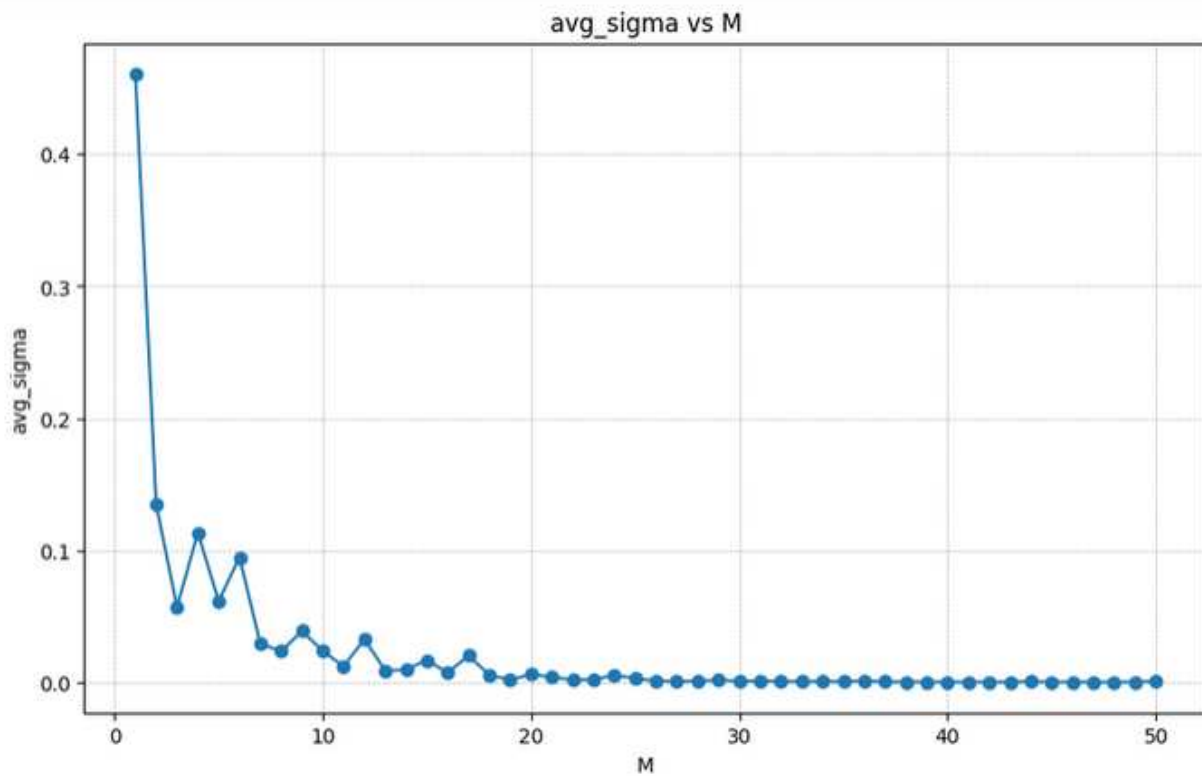


Figure 3.10: Average standard deviation σ as a function of the coupling range M in the locally coupled network Eq. (3.5). Fixed parameters are $a = 0.553$, $\epsilon = 0.0038$, size $N = 100$. The globally coupled limit corresponds to $M = 50$.

3.3.1 Synchronization and range of interaction

Armed with this knowledge, our next aim was to elucidate the interplay between M , ϵ , and synchronization in the locally coupled network Eq. (3.5). The goal is to find how these variables determine the regions of synchronization, contingent on the number of agents and the intensity of the coupling.

Figure 3.11 shows the averaged standard deviation on the space of parameters ($M_{\text{normalized}}$, ϵ) according to a color code, where $M_{\text{normalized}} \equiv 2M/N$. Then, the globally coupled limit corresponds to the value $M_{\text{normalized}} = 1$.

The figure provides a representation of the relationship between the number of neighbors and the coupling strength, tracing the shift from a local coupling to a global coupling as M increases. It becomes evident that the value $\epsilon = 0.0035$ is the threshold for achieving synchronization, a finding consistent with our observations in Figure 3.6. Intriguingly, the data indicates that for successful synchronization, the minimum proportion of agents needed is within the range of 20% of the overall population size N , corroborating insights from Figure 3.10. The chart further emphasizes that increasing the number of neighbors interacting in the coupling, allows for the possibility of a marginally smaller ϵ to instigate synchronization, reflected in a σ value approaching zero. This visualization underscores the intricate dynamics between ϵ and M , identifying the critical values needed for synchronization in the network.

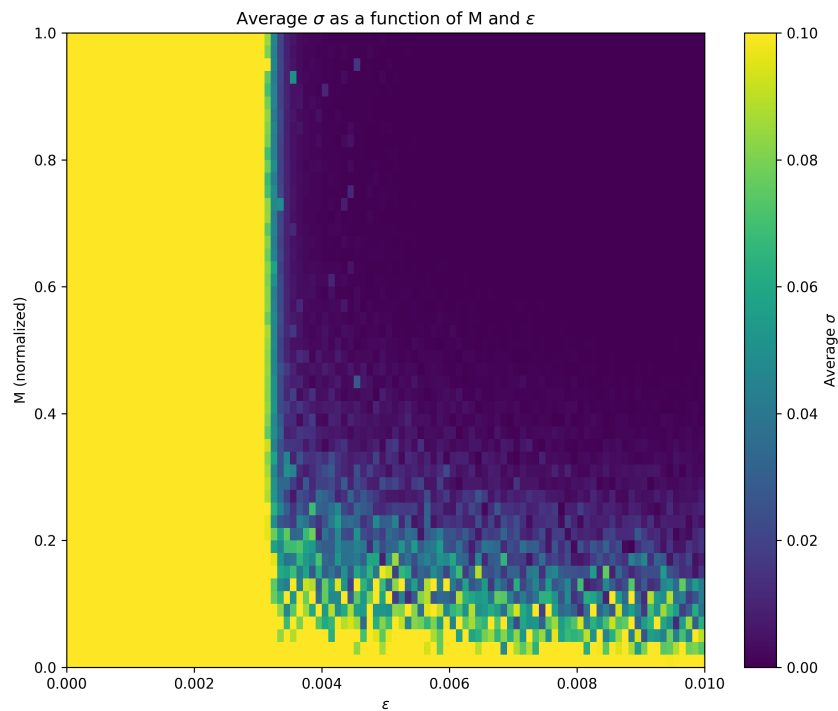


Figure 3.11: Average standard deviation σ as a function of the normalized coupling range $M_{\text{normalized}}$ and the coupling strength ϵ for the locally coupled network Eq. (3.5). Color code is shown on the right bar. Darker regions represent areas of low dispersion or synchronization, while bright regions indicate higher dispersion. This visualization provides insights into the combined effects of local interaction range and coupling strength on the system's dynamics. Fixed parameters are $a = 0.553$, size $N = 100$.

Chapter 4

Conclusions

Collective chaos is a nontrivial collective behavior consisting of the persistence of chaotic behavior at the macroscopic level in systems of interacting dynamical elements possessing individual periodic behavior. This phenomenon is manifested by the existence of chaotic supertransients in time before the system synchronizes into its period attractor. Thus, in practical terms, the observable collective state of the system is spatiotemporal chaos.

In this Thesis we have investigated the role of the connectivity on the emergence of collective chaos in spatiotemporal dynamical networks. Since most studies on this phenomenon have been carried out in coupled map lattices, where time is discrete, we have employed differential equations with continuous time as dynamical units on a coupled network. Furthermore, we have chosen the Linz-Sprott equations which are simplest known nonlinear time-continuous system capable of exhibiting chaos. The Linz-Sprott system possesses a single control parameter which facilitates the search for minimal conditions for observing collective chaos in coupled networks.

Previous studies have shown the emergence of collective chaos mainly in networks with local connections. We have found that collective chaos does not occur in globally coupled networks of continuous time systems, where all elements are coupled together. In this case, synchronization on the periodic orbit of the constitutive elements is achieved. We have characterized the collective synchronized state through a measure of the standard deviation of the states of the elements. Our result indicates that the topology of connectivity of the network is a fundamental factor affecting the occurrence of collective chaos.

On the other hand, we have found that the intensity of the coupling between the elements determines the onset of synchronization. There is a critical value of the coupling parameter above which synchronization occurs and therefore collective chaos collapses.

We have considered a ring network of coupled elements with a varying range of interactions given by the numbers of connected neighbors each element possesses on either side. We have discovered that the range of interactions does play a crucial role on the occurrence of collective chaos. For nearest neighbor couplings collective chaos occurs, in agreement with previous studies. However, there is a critical number of coupled neighbors above which no collective chaos is observed and the network invariably synchronizes in the periodic orbit of the elements.

By normalizing the number of neighbors with respect to the size of the network, we have found that the critical range of interaction for achieving synchronization is about 20% of the size of the network.

The main results of this Thesis are contained in Figure 3.6. This figure unveils the interplay between the intensity of the coupling and the range of interaction required for synchronization in the network.

In summary, our findings illuminate the profound influence that the structure and connectivity of a network have on the emergence of collective behaviors, specifically *spatiotemporal chaos*, in continuous-time dynamical systems. The incorporation of global and local interactions, along with variations in the coupling strength and interaction range, plays a pivotal role in steering the system towards or away from synchronization. Notably, even in scenarios where individual systems exhibit simplistic or predictable behaviors, their collective dynamics can manifest complex patterns, contingent

on the network's architecture. This intricate interplay between individual units and their connectivity has profound implications, especially in real-world systems where heterogeneity and diversity are not exceptions but the norm, such as in ecological, neurological, or social networks.

Bibliography

- [1] Kaneko, K. Supertransients, spatiotemporal intermittency, and stability of fully developed spatiotemporal chaos. *Phys. Lett. A* **1990**, *149*, 105–112.
- [2] González-Estévez, J.; Cosenza, M. G. Network topology and collapse of collective stable chaos. *International Journal of Applied Mathematics and Statistics* **2011**, *26*, 136.
- [3] Linz, S. J.; Sprott, J. Elementary chaotic flow. *Physics Letters A* **1999**, *259*, 240–245.
- [4] Manrubia, S.; Mikhailov, A.; Zanette, D. *Emergence of dynamical order*; World Scientific: Singapore, 2004.
- [5] Kaneko, K.; Tsuda, I. *Complex Systems: Chaos and Beyond*; Springer, 2001.
- [6] Kaneko, K. Globally coupled chaos violates law of large numbers. *Phys. Rev. Lett.* **1990**, *65*, 1391–1394.
- [7] Chaté, H.; Manneville, P. Emergence of effective low-dimensional dynamics in the macroscopic behaviour of coupled map lattices. *Europhys. Lett.* **1992**, *17*, 291–296.
- [8] Cosenza, M. G.; González, J. Synchronization and collective behavior in globally coupled logarithmic maps. *Prog. Theor. Phys.* **1998**, *100*, 21–38.
- [9] Cisneros, L.; Jiménez, J.; Cosenza, M. G.; Parravano, A. Information transfer and nontrivial collective behavior in chaotic coupled map networks. *Physical Review E (Rapid Communications)* **2002**, *65*, 045204(R).
- [10] Politi, A.; Livi, R.; Oppo, G. L.; Kapral, R. Unpredictable behavior in stable systems. *Europhys. Lett.* **1993**, *22*, 571–576.
- [11] Kapral, R.; Livi, R.; Oppo, G.-L.; Politi, A. Dynamics of complex interfaces. *Phys. Rev. E* **1994**, *49*, 2009–2022.
- [12] Kapral, R.; Livi, R.; Oppo, G.-L.; Politi, A. Critical behavior of complex interfaces. *Phys. Rev. Lett.* **1997**, *79*, 2277–2280.
- [13] Wackerbauer, R.; Showalter, K. Collapse of spatiotemporal chaos. *Phys. Rev. Lett.* **2003**, *91*, 174103.
- [14] Wackerbauer, R. Master stability analysis in transient spatiotemporal chaos. *Phys. Rev. E* **2007**, *76*, 056207.
- [15] Wackerbauer, R.; Kobayashi, S. Noise can delay and advance the collapse of spatiotemporal chaos. *Phys. Rev. E* **2007**, *75*, 066209.
- [16] Crutchfield, J. P.; Kaneko, K. Are attractors relevant to turbulence? *Phys. Rev. Lett.* **1988**, *60*, 2715–2718.
- [17] Cecconi, F.; Livi, R.; Politi, A. Fuzzy transition region in a one-dimensional coupled-stable-map lattice. *Phys. Rev. E* **1998**, *57*, 2703–2712.
- [18] Bagnoli, F.; Cecconi, F. Synchronization of non-chaotic dynamical systems. *Phys. Lett A* **2001**, *282*, 9–17.

- [19] Tél, T.; Lai, Y.-C. Chaotic transients in spatially extended systems. *Physics Reports* **2008**, *460*, 245–275.
- [20] Yonker, S.; Wackerbauer, R. Nonlocal coupling can prevent the collapse of spatiotemporal chaos. *Phys. Rev. E* **2006**, *73*, 026218.
- [21] Zillmer, R.; Brunel, N.; Hansel, D. Very long transients, irregular firing, and chaotic dynamics in networks of randomly connected inhibitory integrate-and-fire neurons. *Phys. Rev. E* **2009**, *79*, 031909.
- [22] WMAP Mission Results. <http://map.gsfc.nasa.gov/news/index.html>, 2008.
- [23] Hyman, J.; Nicolaenko, B.; Zaleski, S. Order and complexity in the Kuramoto–Sivashinsky model of weakly turbulent interfaces. *Physica D* **1986**, *23*, 265–292.
- [24] Braun, R.; Feudel, F. Supertransient chaos in the two-dimensional complex Ginzburg–Landau equation. *Phys. Rev. E* **1996**, *53*, 6562–6565.
- [25] Hof, B.; Westerweel, J.; Schneider, T.; Eckhardt, B. Finite lifetime of turbulence in shear flows. *Nature* **2006**, *443*, 59–62.
- [26] Kaneko, K. From globally coupled maps to complex-systems biology. *Chaos: An Interdisciplinary Journal of Nonlinear Science* **2015**, *25*, 097608.
- [27] Cosenza, M. G.; Parravano, A. Dynamics of coupling functions in globally coupled maps: Size, periodicity, and stability of clusters. *Physical Review E* **2001**, *64*, 036224.
- [28] Schimansky-Geier, L. Kuramoto, Y., Chemical Oscillations, Waves, and Turbulence. Berlin-Heidelberg-New York-Tokyo, Springer-Verlag 1984. VIII, 156 S., 41 Abb., DM 79,—. US. 1986.
- [29] Nakagawa, N.; Kuramoto, Y. From collective oscillations to collective chaos in a globally coupled oscillator system. *Physica D: Nonlinear Phenomena* **1994**, *75*, 74–80.
- [30] Grüner, G. The dynamics of charge-density waves. *Reviews of Modern Physics* **1988**, *60*, 1129.
- [31] Wiesenfeld, K.; Hadley, P. Attractor crowding in oscillator arrays. *Physical Review Letters* **1989**, *62*, 1335.
- [32] Wiesenfeld, K.; Bracikowski, C.; James, G.; Roy, R. Observation of antiphase states in a multimode laser. *Physical review letters* **1990**, *65*, 1749.
- [33] Kaneko, K.; Tsuda, I. *Complex Systems: Chaos and Beyond: A Constructive Approach With Applications in Life Sciences*; Springer Science & Business Media, 2001.
- [34] Newman, M. E.; Barabási, A.-L. E.; Watts, D. J. *The structure and dynamics of networks.*; Princeton University Press, 2006.
- [35] Meyers, R. A. *Encyclopedia of complexity and systems science*; Springer New York, 2009; Vol. 9.
- [36] González-Avella, J. C.; Cosenza, M. G.; Tucci, K. Nonequilibrium transition induced by mass media in a model for social influence. *Physical Review E* **2005**, *72*, 065102.
- [37] González-Avella, J. C.; Cosenza, M. G.; Eguíluz, V. M.; San Miguel, M. Spontaneous ordering against an external field in non-equilibrium systems. *New Journal of Physics* **2010**, *12*, 013010.
- [38] González-Avella, J. C.; Cosenza, M. G.; San Miguel, M. Localized coherence in two interacting populations of social agents. *Physica A: Statistical Mechanics and its Applications* **2014**, *399*, 24–30.

- [39] Cosenza, M. G.; Gavidia, M.; González-Avella, J. C. Against mass media trends: Minority growth in cultural globalization. *Plos One* **2020**, *15*, e0230923.
- [40] Garcia-Ojalvo, J.; Elowitz, M. B.; Strogatz, S. H. Modeling a synthetic multicellular clock: repressilators coupled by quorum sensing. *Proceedings of the National Academy of Sciences* **2004**, *101*, 10955–10960.
- [41] Wang, W.; Kiss, I. Z.; Hudson, J. Experiments on arrays of globally coupled chaotic electrochemical oscillators: Synchronization and clustering. *Chaos: An Interdisciplinary Journal of Nonlinear Science* **2000**, *10*, 248–256.
- [42] De Monte, S.; d’Ovidio, F.; Danø, S.; Sørensen, P. G. Dynamical quorum sensing: Population density encoded in cellular dynamics. *Proceedings of the National Academy of Sciences* **2007**, *104*, 18377–18381.
- [43] Taylor, A. F.; Tinsley, M. R.; Wang, F.; Huang, Z.; Showalter, K. Dynamical quorum sensing and synchronization in large populations of chemical oscillators. *Science* **2009**, *323*, 614–617.
- [44] Tinsley, M. R.; Nkomo, S.; Showalter, K. Chimera and phase-cluster states in populations of coupled chemical oscillators. *Nature Physics* **2012**, *8*, 662–665.
- [45] Hagerstrom, A. M.; Murphy, T. E.; Roy, R.; Hövel, P.; Omelchenko, I.; Schöll, E. Experimental observation of chimeras in coupled-map lattices. *Nature Physics* **2012**, *8*, 658–661.

Appendices

Appendix A

Python code for globally coupled network of Linz-Sprott equations

The following code is made in Python.

```
The following code is made in Python.
The globally coupled map network with The local dynamics.
"""@author: David"""
## First we solve one equation in chaotic behavior
#5/09/2023
# First we import lybraries:
import sympy as sp
import numpy as np
import matplotlib.pyplot as plt

#Initial conditions
a = 0.6
h = 0.01
t0 = 0
tf = 40000
t = np.arange(t0, tf+h, h)

# Defining the array resulting function
S = np.array([np.zeros(len(t)),np.zeros(len(t)),np.zeros(len(t))])

#Defining the ODE-function
F = lambda t, s: np.dot(np.array([[0,1,0],[0,0,1],
[0, -1, -a]]), s) + np.array([0 ,0 , np.abs(s[0]) - 1])

#Runge kutta 4
for i in range(len(t)-1):
    k1 = F(t[i], S[:,i])
```

```

k2 = F(t[i] + h/2, S[:,i] + h*k1/2)
k3 = F(t[i] + h/2, S[:,i] + h*k2/2)
k4 = F(t[i] + h, S[:,i] + h*k3)

S[:,i+1] = S[:,i] + (h/6)*(k1 + 2*k2 + 2*k3 + k4)
if np.abs(S[2, i+1]) > 10:
    break

#Define start and end indexes
inicio_idx = int((39500))
fin_idx = int((40000)) + 1

# Plot data over the selected time range
plt.figure(figsize=(18, 13))

# Data series
plt.plot(t[inicio_idx:fin_idx], (S[0]+5)[inicio_idx:fin_idx]
, "b", linestyle='solid', label = r"$x(t) + 5$ (RK4)")
plt.plot(t[inicio_idx:fin_idx], S[1][inicio_idx:fin_idx],
"g", linestyle='solid', label = r"$y(t)$ (RK4)")
plt.plot(t[inicio_idx:fin_idx], (S[2]-4)[inicio_idx:fin_idx],
"r", linestyle='solid', label = r"$z(t) - 4$ (RK4)")

# Labels
plt.xlabel('Time ($t$)', fontsize=28)
plt.ylabel('Functions $x(t), y(t), z(t)$', fontsize=28)

# Adjust tick label size
plt.xticks(fontsize=21)
plt.yticks(fontsize=21)

# Add "a)" label to the top right
plt.annotate('a)', xy=(0.99, 0.99), xycoords='axes fraction',
fontsize=20, ha='right', va='top')

# Legend
plt.legend(fontsize=18, loc="upper left")

# Save and display the graph
plt.savefig("Imagenes/Chaotic_behavior_of_x(t)_y(t)_z(t).png")
plt.show()

## Second we solve one equation in period 3

#Initial conditions
a = 0.553

```

```

h = 0.01
t0 = 0
tf = 40000
t = np.arange(t0, tf+h, h)

# Defining the array resulting function
S = np.array([np.zeros(len(t)),np.zeros(len(t)),np.zeros(len(t))])

#Defining the ODE-function
F = lambda t, s: np.dot(np.array([[0,1,0],[0,0,1],[0, -1, -a]]),
s) + np.array([0 ,0 , np.abs(s[0]) - 1])

#Runge kutta 4
for i in range(len(t)-1):
    k1 = F(t[i], S[:,i])
    k2 = F(t[i] + h/2, S[:,i] + h*k1/2)
    k3 = F(t[i] + h/2, S[:,i] + h*k2/2)
    k4 = F(t[i] + h, S[:,i] + h*k3)

    S[:,i+1] = S[:,i] + (h/6)*(k1 + 2*k2 + 2*k3 + k4)
    if np.abs(S[2, i+1]) > 10:
        break

### Hacemos el acoplamiento con valor  $\epsilon = 0.0001$ 

# Constants
Nit = 100000
Nm = 10
a = 0.553
epsilon = 0.0001
delta_t = 0.05
delta_u0 = 0.6

# Function definition
def f(xyz, u_mean=0):
    x, y, z = xyz

    # Applying matrix transformation
    M = np.array([
        [0, 1, 0],
        [0, 0, 1],
        [0, -1, -a]
    ])
    V = np.array([x, y, z])
    result = np.dot(M, V)

```

```

    # Adding the additional components
    result += (1 - epsilon) * np.array([0, 0, np.abs(x) - 1])
    + epsilon * np.array([0, 0, u_mean])

    return result

# Initialization
u0 = np.array([0.3077, -0.8528, -0.1290]) + np.random.uniform
(-delta_u0, delta_u0, (Nm, 3))
Sold = np.zeros((Nit, Nm, 3))
fmean = np.zeros(Nit)

# Main loop
for n in range(Nit):
    Sold[n] = u0
    ui = []
    u_mean = np.mean(u0[:,2])
    for i in range(Nm):
        k1 = delta_t * f(u0[i], u_mean)
        k2 = delta_t * f(u0[i] + 0.5 * k1, u_mean)
        k3 = delta_t * f(u0[i] + 0.5 * k2, u_mean)
        k4 = delta_t * f(u0[i] + k3, u_mean)
        ui.append(u0[i] + 1 / 6 *
            (k1 + 2 * k2 + 2 * k3 + k4))

    ui = np.array(ui)
    um = np.mean(ui[:,2])
    fmean[n] = um
    u = (1 - epsilon) * ui + epsilon *
    np.array([[0, 0, um]] * Nm)
    u0 = u
    # Calcula las medias de x y y para cada paso de tiempo
    x_mean = np.mean(Sold[:, :, 0], axis=1)
    y_mean = np.mean(Sold[:, :, 1], axis=1)

# Create time vector
t = np.arange(0, Nit)

# Set the figure size
plt.figure(figsize=(18, 12)) # Adjust width and height as needed

# Define indices for the time range
inicio_idx = 98000
fin_idx = 100000

# Plot individual z functions for specified time range
for i in range(Nm):

```

```
plt.plot(t[inicio_idx:fin_idx], Sold[inicio_idx:fin_idx, i, 2],
label=f'z_{i}(t)')

# Plot mean z function for specified time range
plt.plot(t[inicio_idx:fin_idx], fmean[inicio_idx:fin_idx], 'k',
linewidth=3, label='z_mean(t)')

# Labels
plt.xlabel('Time ($t$)', fontsize=22)
plt.ylabel('z_i(t), z_mean(t)', fontsize=22)

# Adjust tick label size
plt.xticks(fontsize=18)
plt.yticks(fontsize=18)

# Add "b)" label to the top right
plt.annotate('b)', xy=(0.99, 0.99), xycoords='axes fraction', fontsize=20,
ha='right', va='top')

# Legend
plt.legend(fontsize=16, loc="upper left")

# Ensure everything fits well
plt.tight_layout()

# Adjust the plot to prevent clipping
plt.subplots_adjust(bottom=0.15) # Ajusta el 0.15 según sea necesario

# Save the figure to a file before displaying it
plt.savefig("Imagenes/Evolution_of_z_functions.png", bbox_inches='tight')

# Display the figure
plt.show()

## We define a function for epsilon

def simulate_for_epsilon(epsilon):

    # Constants
    Nit = 20000
    Nm = 100
    a = 0.553
    delta_t = 0.05
    delta_u0 = 0.5
    p = 0.25
```

```

# Function definition
def f(u):
    x, y, z = u
    return np.array([y, z, -a*z - y + abs(x) - 1])

def F(u):
    k1 = f(u)
    k2 = f(u + 0.5 * delta_t * k1)
    k3 = f(u + 0.5 * delta_t * k2)
    k4 = f(u + delta_t * k3)
    return (1/6.0) * delta_t * (k1 + 2*k2 + 2*k3 + k4)

# Initialization
u0 = np.random.uniform(-delta_u0, delta_u0, (Nm, 3))
Sold = []
fmean = []
sigma = []

# Main loop
for n in range(Nit):
    Sold.append(np.copy(u0))
    ui = np.array([u + F(u) for u in u0])
    um = np.mean(ui[:, 2])
    fmean.append(um)
    sigma.append(np.std(ui[:, 2]))

    if np.random.rand() <= p:
        u = (1-epsilon) * ui + epsilon *
            np.array([[0,0,um] for _ in range(Nm)])
    else:
        u = (1-epsilon) * ui + epsilon *
            np.array([[0,0,um] for _ in range(Nm)])

    if um < -100 or um > 100:
        break
    u0 = u

# Descartar los primeros 2000 valores y sumar el resto
sum_sigma = sum(sigma[2000:])

# Calcular el promedio dividiendo por 8000
avg_sigma = sum_sigma / 8000

return avg_sigma

# Rango de valores de epsilon

```

```

epsilons = np.linspace(0, 0.01, 50)
epsilons = np.round(epsilons, 5)
avg_sigmas = [simulate_for_epsilon(epsilon) for epsilon in epsilons]

# Gráfica de avg_sigma vs epsilon
plt.figure(figsize=(10,6))
plt.plot(epsilons, avg_sigmas, '-o', label='avg_sigma')
plt.xlabel('epsilon')
plt.ylabel('avg_sigma')
plt.legend()
plt.grid(True)
plt.title('avg_sigma vs epsilon')
plt.show()

## Now for the local dynamics
import numpy as np
import matplotlib.pyplot as plt

Nit = 10000
Nm = 100
M = 2
a = 0.553
epsilon = 0.004
delta_t = 0.05
delta_u0 = 0.5
u0 = np.random.uniform(-delta_u0, delta_u0, (Nm, 3))

def f(u):
    return np.array([u[1], u[2], -a*u[2] - u[1] + abs(u[0]) - 1])

def F(u):
    k1 = f(u)
    k2 = f(u + 0.5 * delta_t * k1)
    k3 = f(u + 0.5 * delta_t * k2)
    k4 = f(u + delta_t * k3)
    return (1/6.0) * delta_t * (k1 + 2*k2 + 2*k3 + k4)

Sold = []
fmean = []
sigma = []

for n in range(Nit):
    Sold.append(u0)

    ui = np.array([u0[i] + F(u0[i]) for i in range(Nm)])
    uj = np.concatenate((u0[-M:], u0, u0[:M]))

```

```

um = np.array([1/(2.0*M + 1) *
np.sum(uj[j-M:j+M+1, 2]) for j in range(M, M+Nm)])
umean = np.mean(ui[:,2])
fmean.append(umean)
sigma.append(np.std(ui[:,2]))

u = (1-epsilon)*ui + epsilon*np.array([[0,0,um_i] for um_i in um])

if any(val > 100 or val < -100 for val in um):
    break

u0 = u

# Create time vector
t = np.arange(0, Nit)

# Define indices for the time range
inicio_idx = 8000
fin_idx = 10000

# Plotting
plt.figure(figsize=(14, 12))

# Create a new range for x-axis to reflect
the number of data points being plotted
x_range = range(fin_idx - inicio_idx)

colors = ['blue', 'green', 'red']
# Define a list of colors for better distinction

for i in range(3):
    plt.plot(x_range,
             [sold[i][2] for sold in Sold[inicio_idx:fin_idx]],
             color=colors[i],
             label=f'z_{i}(t)') # Add label for each z_i(t)

plt.plot(x_range, fmean[inicio_idx:fin_idx], 'k',
         linewidth=3, label='z_mean(t)')
plt.xlabel('Time (t)')
plt.ylabel('z_i(t) and Mean z')
plt.title
('Globally coupled time evolution of individual z-values and z-mean')

plt.legend()
plt.grid(True)

```

```

plt.tight_layout()

# Guardar el gráfico
plt.savefig("Imágenes/Time_Evolution_of_z_Values.png", dpi=300) Appendix A
Python code for globally coupled network of
Linz-Sprott equations

#Initial conditions
a = 0.6
h = 0.01
t0 = 0
tf = 40000
t = np.arange(t0, tf+h, h)
# Defining the array resulting function
S = np.array([np.zeros(len(t)),
np.zeros(len(t)),np.zeros(len(t))])
#Defining the ODE-function
F = lambda t, s:
np.dot(np.array([[0,1,0],[0,0,1],[0, -1, -a]]), s)
+ np.array([0 ,0 , np.abs(s[0]) - 1
#Runge kutta 4
for i in range(len(t)-1):
k1 = F(t[i], S[:,i])
k2 = F(t[i] + h/2, S[:,i] + h*k1/2)
k3 = F(t[i] + h/2, S[:,i] + h*k2/2)
k4 = F(t[i] + h, S[:,i] + h*k3)

S[:,i+1] = S[:,i] + (h/6)*(k1 + 2*k2 + 2*k3 + k4)
if np.abs(S[2, i+1]) > 10:
break
#Define start and end indexes
inicio_idx = int((39500))
fin_idx = int((40000)) + 1
# Plot data over the selected time range
plt.figure(figsize=(18, 13))
# Data series
plt.plot(t[inicio_idx:fin_idx],
(S[0]+5)[inicio_idx:fin_idx], "b", linestyle='solid', label = r"$x(t)$")
plt.plot(t[inicio_idx:fin_idx],
S[1][inicio_idx:fin_idx], "g", linestyle='solid', label = r"$y(t)$ (RK")
plt.plot(t[inicio_idx:fin_idx],
(S[2]-4)[inicio_idx:fin_idx], "r", linestyle='solid', label = r"$z(t)$")
# Labels
plt.xlabel('Time ($t$)', fontsize=28)
plt.ylabel('Functions $x(t)$, $y(t)$, $z(t)$', fontsize=28)
# Adjust tick label size

```

```

plt.xticks(fontsize=21)
plt.yticks(fontsize=21)
# Add "a)" label to the top right
plt.annotate('a)', xy=(0.99, 0.99),
xycoords='axes fraction', fontsize=20, ha='right', va='top')
# Legend
plt.legend(fontsize=18, loc="upper left")
# Save and display the graph
plt.savefig("Imagenes/Chaotic_behavior_of_x(t)_y(t)_z(t).png")
plt.show()
## Second we solve one equation in period 3
#Initial conditions
a = 0.553
h = 0.01
t0 = 0
tf = 40000
t = np.arange(t0, tf+h, h)
# Defining the array resulting function
S = np.array([np.zeros(len(t)),np.zeros(len(t)),np.zeros(len(t))])

```

School of Physical Sciences and Nanotechnology UNIVERSITY YACHAY TECH

```

#Defining the ODE-function
F = lambda t, s:
np.dot(np.array([[0,1,0],[0,0,1],[0, -1, -a]]), s)
+ np.array([0 ,0 , np.abs(s[0]) - 1
#Runge kutta 4
for i in range(len(t)-1):
k1 = F(t[i], S[:,i])
k2 = F(t[i] + h/2, S[:,i] + h*k1/2)
k3 = F(t[i] + h/2, S[:,i] + h*k2/2)
k4 = F(t[i] + h, S[:,i] + h*k3)
S[:,i+1] = S[:,i] + (h/6)*(k1 + 2*k2 + 2*k3 + k4)
if np.abs(S[2, i+1]) > 10:
break
# Constants
Nit = 100000
Nm = 10
a = 0.553
epsilon = 0.0001
delta_t = 0.05
delta_u0 = 0.6
# Function definition
def f(xyz, u_mean=0):
x, y, z = xyz
# Applying matrix transformation
M = np.array([

```

```

[0, 1, 0],
[0, 0, 1],
[0, -1, -a]
])
V = np.array([x, y, z])
result = np.dot(M, V)
# Adding the additional components
result += (1 - epsilon) * np.array([0, 0, np.abs(x) - 1])
+ epsilon * np.array([0, 0, u_mean])
return result
# Initialization
u0 = np.array([0.3077, -0.8528, -0.1290])
+ np.random.uniform(-delta_u0, delta_u0, (Nm, 3))
Sold = np.zeros((Nit, Nm, 3))
fmean = np.zeros(Nit)

#Initial conditions
a = 0.6
h = 0.01
t0 = 0
tf = 40000
t = np.arange(t0, tf+h, h)
# Defining the array resulting function
S = np.array([np.zeros(len(t)),
np.zeros(len(t)),np.zeros(len(t))])
#Defining the ODE-function
F = lambda t, s:
np.dot(np.array([[0,1,0],[0,0,1],[0, -1, -a]]), s)
+ np.array([0 ,0 , np.abs(s[0]) - 1
#Runge kutta 4
for i in range(len(t)-1):
k1 = F(t[i], S[:,i])
k2 = F(t[i] + h/2, S[:,i] + h*k1/2)
k3 = F(t[i] + h/2, S[:,i] + h*k2/2)
k4 = F(t[i] + h, S[:,i] + h*k3)
S[:,i+1] = S[:,i] + (h/6)*(k1 + 2*k2 + 2*k3 + k4)
if np.abs(S[2, i+1]) > 10:
break
#Define start and end indexes
inicio_idx = int((39500))
fin_idx = int((40000)) + 1
# Plot data over the selected time range
plt.figure(figsize=(18, 13))
# Data series
plt.plot(t[inicio_idx:fin_idx],
(S[0]+5)[inicio_idx:fin_idx], "b", linestyle='solid', label = r"$x(t)$")

```

```

plt.plot(t[inicio_idx:fin_idx],
S[1][inicio_idx:fin_idx], "g", linestyle='solid', label = r"$y(t)$ (RK
plt.plot(t[inicio_idx:fin_idx],
(S[2]-4)[inicio_idx:fin_idx], "r", linestyle='solid', label = r"$z(t)
# Labels
plt.xlabel('Time ($t$)', fontsize=28)
plt.ylabel('Functions $x(t), y(t), z(t)$', fontsize=28)
# Adjust tick label size
plt.xticks(fontsize=21)
plt.yticks(fontsize=21)
# Add "a" label to the top right
plt.annotate('a', xy=(0.99, 0.99),
xycoords='axes fraction', fontsize=20, ha='right', va='top')
# Legend
plt.legend(fontsize=18, loc="upper left")
# Save and display the graph
plt.savefig("Imagenes/Chaotic_behavior_of_x(t)_y(t)_z(t).png")
plt.show()
## Second we solve one equation in period 3
#Initial conditions
a = 0.553
h = 0.01
t0 = 0
tf = 40000
t = np.arange(t0, tf+h, h)
# Defining the array resulting function
S = np.array([np.zeros(len(t)),
np.zeros(len(t)),np.zeros(len(t))])

F = lambda t, s: np.dot(np.array([[0,1,0],[0,0,1],
[0, -1, -a]]), s) + np.array([0 ,0 , np.abs(s[0]) - 1
#Runge kutta 4
for i in range(len(t)-1):
k1 = F(t[i], S[:,i])
k2 = F(t[i] + h/2, S[:,i] + h*k1/2)
k3 = F(t[i] + h/2, S[:,i] + h*k2/2)
k4 = F(t[i] + h, S[:,i] + h*k3)
S[:,i+1] = S[:,i] + (h/6)*(k1 + 2*k2 + 2*k3 + k4)
if np.abs(S[2, i+1]) > 10:
break
### Hacemos el acoplamiento con valor $\epsilon = 0.0001$
# Constants
Nit = 100000
Nm = 10
a = 0.553
epsilon = 0.0001

```

```

delta_t = 0.05
delta_u0 = 0.6
# Function definition
def f(xyz, u_mean=0):
    x, y, z = xyz
    # Applying matrix transformation
    M = np.array([
        [0, 1, 0],
        [0, 0, 1],
        [0, -1, -a]
    ])
    V = np.array([x, y, z])
    result = np.dot(M, V)
    # Adding the additional components
    result += (1 - epsilon) * np.array([0, 0, np.abs(x) - 1])
    + epsilon * np.array([0, 0, u_mean])
    return result
# Initialization
u0 = np.array([0.3077, -0.8528, -0.1290])
+ np.random.uniform(-delta_u0, delta_u0, (Nm, 3))
Sold = np.zeros((Nit, Nm, 3))
fmean = np.zeros(Nit)
Physicist 43 Final Grade Project

plt.show()

# Plotting standard deviation
plt.figure(figsize=(10, 5))
plt.plot(range(len(sigma)), sigma, color='red')
plt.xlabel('Time')
plt.ylabel('Standard Deviation')
plt.grid(True, which='both', linestyle='--', linewidth=0.5)
plt.title('Standard Deviation over Time')

# Guardar el gráfico
plt.savefig("Imagenes/Standard_Deviation_over_Time.png", dpi=300)

plt.show()

# Descartar los primeros 2000 valores y sumar el resto
sum_sigma = sum(sigma[2000:])

# Calcular el promedio dividiendo por 8000
avg_sigma = sum_sigma / 8000

```

```

print(avg_sigma)

## We define a function for M

def run_simulation(M):
    Nit = 25000
    Nm = 100
    a = 0.553
    epsilon = 0.0038
    delta_t = 0.05
    delta_u0 = 0.5
    u0 = np.random.uniform(-delta_u0, delta_u0, (Nm, 3))

    def f(u):
        return np.array([u[1], u[2], -a*u[2] - u[1] + abs(u[0]) - 1])

    def F(u):
        k1 = f(u)
        k2 = f(u + 0.5 * delta_t * k1)
        k3 = f(u + 0.5 * delta_t * k2)
        k4 = f(u + delta_t * k3)
        return (1/6.0) * delta_t * (k1 + 2*k2 + 2*k3 + k4)

    sigma = []

    for n in range(Nit):
        ui = np.array([u0[i] + F(u0[i]) for i in range(Nm)])
        uj = np.concatenate((u0[-M:], u0, u0[:M]))

        um = np.array([1/(2.0*M + 1) *
            np.sum(uj[j-M:j+M+1, 2]) for j in range(M, M+Nm)])

        if any(val > 100 or val < -100 for val in um):
            break

        sigma.append(np.std(ui[:,2]))

        u0 = (1-epsilon)*ui +
            epsilon*np.array([[0,0,um_i] for um_i in um])

    # Descartar los primeros 2000 valores y sumar el resto
    sum_sigma = sum(sigma[3000:])
    avg_sigma = sum_sigma / 22000

    return avg_sigma

```

```

# Ejecuta la simulación para diferentes valores de M
M_values = list(range(0, 51))
avg_sigma_values = [run_simulation(M) for M in M_values]

# Haz un plot de los resultados
plt.figure(figsize=(10, 6))
plt.plot(M_values, avg_sigma_values, '-o')
plt.xlabel('M')
plt.ylabel('avg_sigma')
plt.title('avg_sigma vs M')
plt.grid(True, which='both', linestyle='--', linewidth=0.5)
plt.show()

## Fusiona las dos funciones para
simular con un epsilon y M específicos

def simulate_for_epsilon_and_M(epsilon, M):

    Nit = 20000
    Nm = 100
    a = 0.553
    delta_t = 0.05
    delta_u0 = 0.5

    # Function definition
    def f(u):
        x, y, z = u
        return np.array([y, z, -a*z - y + abs(x) - 1])

    def F(u):
        k1 = f(u)
        k2 = f(u + 0.5 * delta_t * k1)
        k3 = f(u + 0.5 * delta_t * k2)
        k4 = f(u + delta_t * k3)
        return (1/6.0) * delta_t * (k1 + 2*k2 + 2*k3 + k4)

    # Initialization
    u0 = np.random.uniform(-delta_u0, delta_u0, (Nm, 3))
    sigma = []

    for n in range(Nit):
        ui = np.array([u0[i] + F(u0[i]) for i in range(Nm)])
        uj = np.concatenate((u0[-M:], u0, u0[:M]))

        um = np.array([1/(2.0*M + 1)

```

```

    * np.sum(uj[j-M:j+M+1, 2]) for j in range(M, M+Nm)])

if any(val > 100 or val < -100 for val in um):
    break

sigma.append(np.std(ui[:,2]))

u0 = (1-epsilon)*ui
+ epsilon*np.array([[0,0,um_i] for um_i in um])

# Descartar los primeros 2000 valores y sumar el resto
sum_sigma = sum(sigma[2000:])
avg_sigma = sum_sigma / 8000

return avg_sigma

# Rango de valores
epsilon = np.linspace(0, 0.01, 100)
M_values = list(range(1, 51))

# Crear una matriz 2D para almacenar los valores de sigma
sigma_matrix = np.zeros((len(M_values), len(epsilon)))

# Llenar la matriz con valores de sigma para cada par (M, epsilon)
for i, M in enumerate(M_values):
    for j, epsilon in enumerate(epsilon):
        sigma_matrix[i, j] = simulate_for_epsilon_and_M(epsilon, M)

# Visualizar la matriz como un mapa de calor
plt.imshow(sigma_matrix, origin='lower', aspect='auto',
extent=[epsilon[0], epsilon[-1],
M_values[0], M_values[-1]], cmap='viridis')
plt.colorbar(label='Average Sigma')
plt.xlabel('Epsilon')
plt.ylabel('M')
plt.title('Average Sigma as a function of M and Epsilon')
plt.show()

```